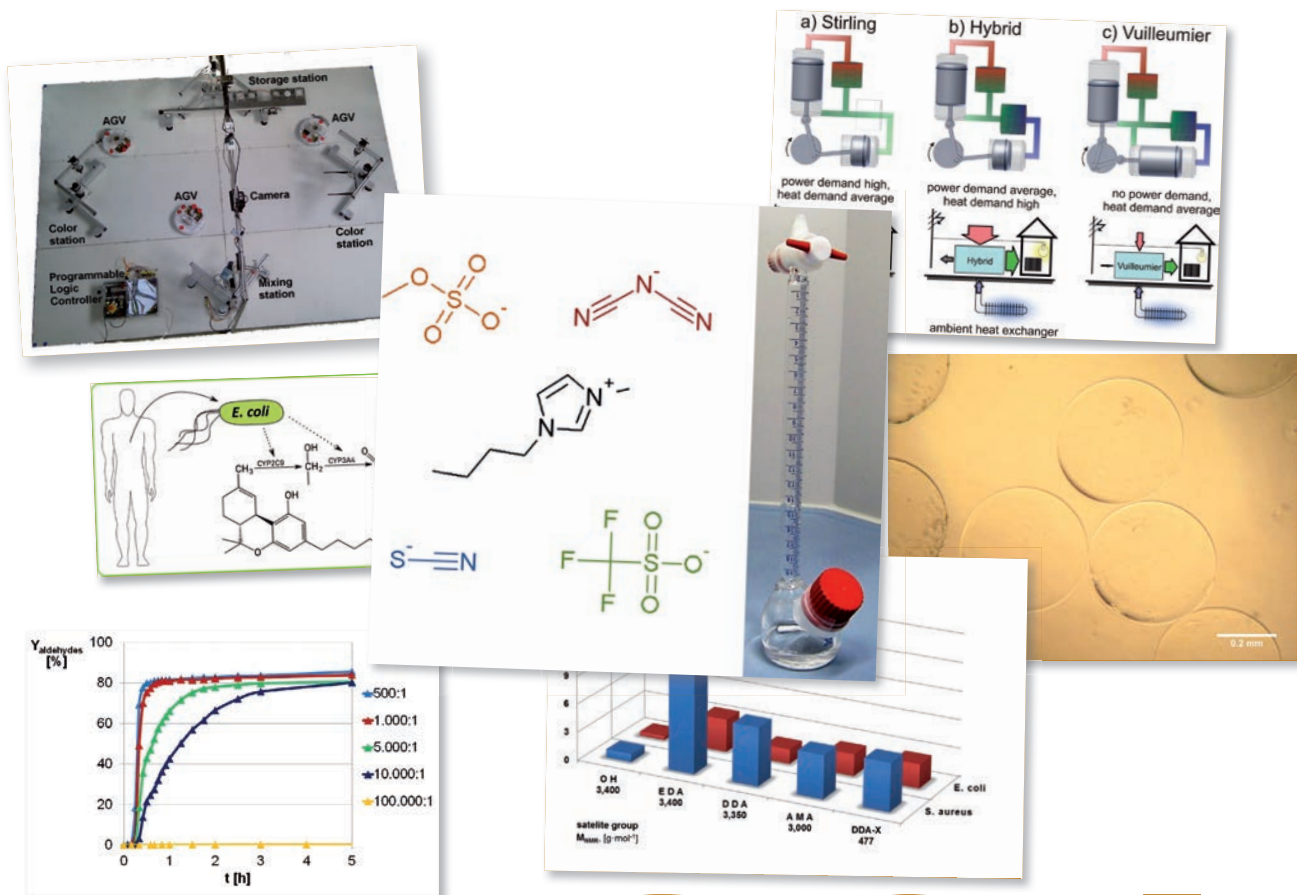


# SCIENTIFIC HIGHLIGHTS

## Annual Report



# 2011

---

## Content

---

|   |           |
|---|-----------|
| <b>Department of BCI</b>  | <b>4</b>  |
| Preface   | 5         |
| <br>  |           |
| <b>Equipment Design (AD)</b>  | <b>6</b>  |
| Flow Phenomena and Mixing in Curved Microchannels   | 7         |
| Scale-up concept of microstructured reactors  | 8         |
| <br>  |           |
| <b>Plant and Process Design (APT)</b>   | <b>10</b> |
| Methodology for the Reduction of Energy Consumption of process plants                                       | 11        |
| Sequential model parameter determination procedure to simulate induced nucleation crystallization processes | 12        |
| <br>  |           |
| <b>Biomaterials and Polymer Science (BMP)</b>   | <b>14</b> |
| Stress-induced melting of crystals in natural rubber  | 15        |
| Polymer Enzyme conjugates with Poly(oxazoline)s   | 16        |
| Amphiphilic Poly(2-oxazoline) ABA-Triblock Copolymers   | 17        |
| Biocidal Polymers with Satellite Groups   | 18        |
| APCN for activating enzymes in organic solvents   | 19        |
| <br>  |           |
| <b>Chemical Biotechnology (BT)</b>  | <b>20</b> |
| Anaerobic Carbon Oxyfunctionalization   | 21        |
| Towards a constitutive solvent tolerant phenotype of <i>Pseudomonas</i> sp. strain VLB120                   | 22        |
| Improved proline 4-hydroxylase (P4H) by random mutagenesis  | 23        |
| Segmented flow biofilm membrane microreactors   | 24        |
| Single Cell Analysis with Picoliter nDEP Traps  | 25        |
| <br>  |           |
| <b>Biochemical Engineering (BVT)</b>  | <b>26</b> |
| Biopolymer immobilization of enzymes  | 27        |
| Biobutanol Production   | 28        |
| <br>  |           |
| <b>Process Dynamics and Operations (DYN)</b>  | <b>30</b> |
| Realization of NMPC in an Industrial Polymerization Process   | 31        |
| Timed Automata Based Scheduling for a Miniature Pipeless Plant with Mobile Robots                           | 32        |
| <br>  |           |
| <b>Fluid Separations (FVT)</b>  | <b>34</b> |
| Membrane-Assisted Reactive Separation Processes   | 35        |
| Aqueous two-phase extraction of monoclonal antibodies   | 36        |
| Ionic Liquids   | 37        |

---

## Content

---

|  |           |
|--|-----------|
| <b>Mechanical Process Engineering (MV)</b>   | <b>38</b> |
| Characterization of dynamic mixers by the optical measurement of droplet size distributions of emulsions | 39        |
| CFD-Simulation of the electrostatic precipitation process  | 40        |
| Particle Classification in a high viscous environment  | 41        |
| Wet Scrubber Simulation  | 42        |
| <br>   |           |
| <b>Technical Biochemistry (TB)</b>   | <b>44</b> |
| Towards a platform organism for terpenoid production   | 45        |
| Human tetrahydrocannabinol metabolites   | 46        |
| <br>   |           |
| <b>Technical Chemistry A (TCA)</b>   | <b>48</b> |
| Homogeneously catalysed Hydroformylation of 1-Dodecene   | 49        |
| Cross metathesis of methyl undec-10-enoate with dimethyl maleate   | 50        |
| Homogeneous catalysed alkoxy-carbonylation of myrcene  | 51        |
| Catalytic hydrogenation of carbon dioxide to formic acid   | 52        |
| Efficient Hydroformylation of 1,3-Pentadiene   | 53        |
| <br>   |           |
| <b>Technical Chemistry B (TCB)</b>   | <b>54</b> |
| Resource efficiency by using CO <sub>2</sub> as a raw material   | 55        |
| Selectivity enhancement by using permselective microcapsule  | 56        |
| Slug flow of ionic liquids in capillary microcontactors  | 57        |
| <br>   |           |
| <b>Thermodynamics (TH)</b>   | <b>58</b> |
| Solubility of Pharmaceuticals  | 59        |
| Thermodynamic Characterization of Membrane Materials   | 60        |
| Modeling Weak-Electrolyte Solutions  | 61        |
| Decentralized Energy Supply for Domestic Applications  | 62        |



**Department of BCI**

## Preface

---

Dear Readers,

After the first presentation of our scientific highlights of 2010, we have got very positive response from our academic and industrial partners as well as from our students.

Therefore, we have decided to present our colorful research potpourri in the new scientific highlights of 2011. This year was full of exciting events, crowned with the Gottfried-Wilhelm-Leibniz-Preis to Prof. Gabriele Sadowski, indicating the great scientific impact of the BCI on the engineering community. The presented abstracts are not covering all research activities, but only the most successful ones.

Each research project has the contact information attached and we encourage interested persons of academic or industrial background, but also high school students to contact us for questions or ideas.

We hope that this brochure will be of interest to everyone, who is intrigued by the many facets of our research. It is also supposed to work as guide for students to find their best suited research topic for the bachelor, master or the Ph.D. thesis.

Enjoy the reading.



## Equipment Design (AD)

## Flow Phenomena and Mixing in Curved Microchannels

### Process intensification in microreactors

Norbert Kockmann, Maximilian Fischer

In microchannels with typical dimensions from 10  $\mu\text{m}$  to few hundreds  $\mu\text{m}$ , the flow is dominated by viscous forces, often leading to laminar flow conditions. At the entrance or in bends and curves, where the flow changes its velocity or direction, inertial forces generate transverse flow velocities. Vortex pairs are generated by Dean flow in circular bends, which are still laminar, steady, and showing no statistically distributed fluctuations typical for turbulent flow, see Fig. 1. This deviation from straight laminar conditions is called transitional flow, often occurring in channels larger than 500  $\mu\text{m}$  at higher flow rates.

Transitional flow phenomena include the first occurrence of flow bifurcation, pulsating vortices, period doubling of vortex pairs, and regularly fluctuating wake flow or vortex shedding. Chaotic flow phenomena are the first evidence of turbulence. Transitional flow augments the transport characteristics in microchannels for enhanced heat and mass transfer and for performing chemical reactions in microreactors.

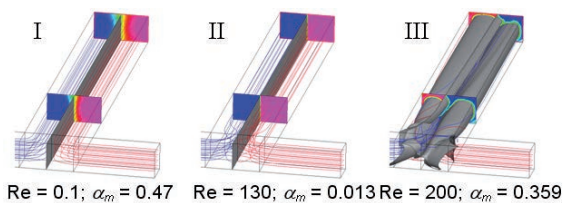


**Figure 1:** Overview of the flow regimes in laminar and transitional T-joint flow with 1:1 mixing ratio,  $Sc = 3700$ , mixing quality  $\alpha$  as normalized standard deviation of the concentration field at the outlet of the mixing channel in a T-shaped micromixer 300  $\mu\text{m}$  deep, 300  $\mu\text{m}$  wide inlet, and 600  $\mu\text{m}$  wide mixing channel.

Heat and mass transfer in microchannels are determined by the fluid dynamics. Miniaturized channels improve the heat transfer and mixing, but are dominated by viscous forces leading to laminar flow. To overcome hindered transport in laminar flow, vortices and other secondary flow structures can be induced within the channel elements, bends, curves, and inserts augmenting the lateral transport

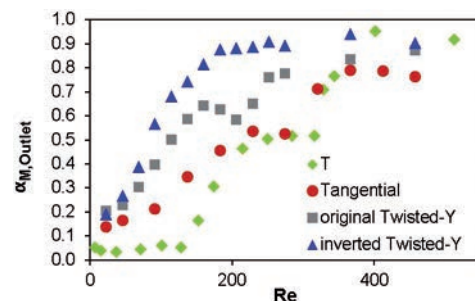


**Figure 2:** Mixing quality  $\alpha$  over Reynolds number at outlet of original and inverted Twisted-Y mixer, T-mixer and Tangential mixer.

A CFD study was performed starting from a T-mixer and a Tangential mixer. The contact element was varied from Twisted-Y mixer (Fig. 3) to 60° Y mixer. The mixing channel was always an SZ-shaped meandering channel. The mixing quality significantly increases by a factor of 2 to more than 5 compared to the T-shaped mixer, see Fig. 2. Experimental data confirm the mixing enhancement in curved microchannels.

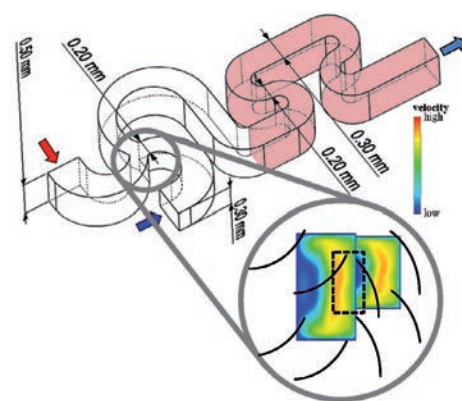


**Figure 3:** Geometry of original Twisted-Y mixer and flow distribution in the contacting region.

Publications:  
 N. Kockmann, D.R. Roberge, Transitional Flow and Related Transport Phenomena in Curved Microchannels, *Heat Transfer Engineering*, 32, 595-608, 2011.  
 C. Holvey, et al. Pressure drop and mixing in single phase microreactors: Simplified designs of micromixers, *Chem. Eng. & Proc.* 50, 1069-1075, 2011

## Scale-up concept of microstructured reactors

*From lab to production with continuous-flow processes*

Norbert Kockmann

Microstructured reactors are characterized by rapid mixing processes and excellent temperature control of chemical reactions. These properties allow the safe operation of hazardous chemistry in intensified processes. Problems occur during scale-up of these processes, where heat transfer becomes the limiting effect. With high flow rates and transitional or even turbulent flow regimes in small channels, rapid mixing and excellent heat transfer can be maintained up to high production rates.

Exothermic reactions are limited by parametric sensitivity and safe operation are shown from literature and combined with convective heat transfer for consistent scale-up. Good knowledge of reaction kinetics, thermodynamics and heat transfer is essential to determine runaway regions for exothermic reactions. From these correlations, consistent channel design and continuous-flow reactor setup is shown. Fig. 1 displays the main scale-up parameters for microstructured, continuous-flow reactors.

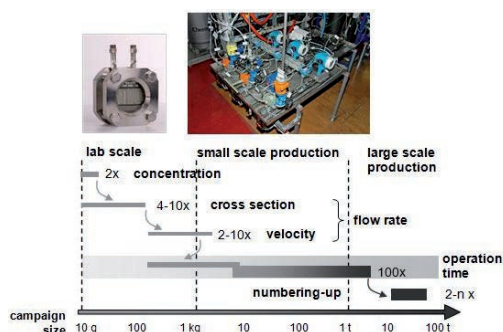


**Figure 1:** Scale-up parameters and their telescoping range for continuous-flow reactors, images are taken from the Lonza Flow-Plate™ concept.

The flow rate through the reactor can be increased by larger cross section or higher flow rate. One key factor of the reactor scale-up is the specific channel arrangement with mixing and residence time segments, which provide geometrical similarity over the entire scale. The main leverage to increase the throughput is the operational time, determined by the environment of the plant setup and material logistics. For even higher production rates, parallelization of equipment can be considered.

The characteristic dimension, the hydraulic diameter, is scaled-up for constant mixing time and heat transfer characteristics. In the laminar flow regime, the hydraulic diameter for constant mixing and heat transfer correlates with the volumetric flow rate to

$$d_h \propto \dot{V}^{1/3} \quad d_h \propto \dot{V}^{1/7}$$

respectively. For the turbulent regime, the following correlations were found

$$d_h \propto \dot{V}^{3/7} \quad d_h \propto \dot{V}^{2/7}$$

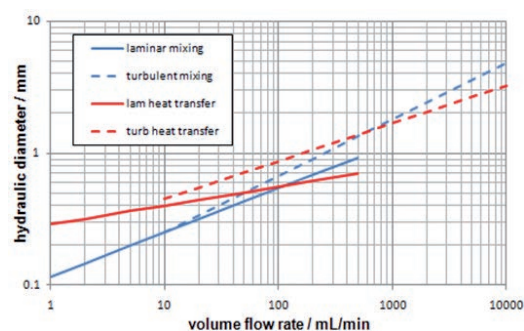


**Figure 2:** Scale-up of typical hydraulic diameter for mixing (blue) and heat transfer (red) from parametric sensitivity in laminar (straight line) and turbulent flow regime (dotted line).

For strong exothermic reactions, the parametric sensitivity and reactor stability is a crucial issue, which can be described by three different approaches. Based on dimensionless numbers for reaction kinetics and thermodynamics, correlations are derived including also convective heat transfer for safe operation conditions. The correlations for channel scale-up considering convective heat transfer as well as external heat transfer resistance are integrated in a generic design and process development procedure. Simple and robust scale-up with equipment modularity for multipurpose applications will give new drive for microreactor development and applications. Nevertheless, experimental case studies to validate the presented correlations are very important and the goal of ongoing and future work.

Contact:  
norbert.kockmann@udo.edu

### Publications:

N. Kockmann, M. Gottsponer, D.M. Roberge, Scale-up Concept of Single-Channel Microreactors from Process Development to Industrial Production, Chem. Eng. J. 167, 718-726, 2011.  
N. Kockmann, D.R. Roberge, Scale-up concept for modular microstructured reactors based on mixing, heat transfer, and reactor safety. Chem. Eng. & Proc. 50, 1017-1026, 2011.





## Plant and Process Design (APT)

## Methodology for the Reduction of Energy Consumption of process plants

Christian Dowidat, Christian Bramsiepe, Gerhard Schembecker

*While prevention of the global warming and climate change is one of the major challenges in this century, carbon dioxide emissions were identified as main contributors for global warming. One opportunity to reduce carbon dioxide emissions is the efficient use of energy. A positive side effect of the decrease of energy consumption is the reduction of operating costs. While energy efficiency optimizations are already widely applied in continuous processes (e.g. pinch analysis for heat integration) batch processes are rarely taken into consideration. In this work measures for energy efficiency increase of process plants are investigated with a focus on batch processes.*

Energy losses can be described as the difference between energy consumption of a present process and the corresponding (energetically) optimal process. Energetic losses can be divided into static and dynamic losses, where static losses are a result of the technical implementation of the process. These could be heat losses due to insufficient insulation or the application of energy intensive unit operations. Dynamic losses are caused by suboptimal operation of the plant. In this study, heuristics are developed to reduce both static and dynamic losses.

These heuristics lead to proposals for measures to increase energy efficiency of a process. In most cases an investment has to be made (e.g. for new apparatuses) to realize such measures. The amount of this investment and the value of resulting energy savings determine whether an investment is taken or not. But both, necessary investment and resulting savings, depend on the timing of the investment. At this, investment costs vary because of the varying prices of materials and the savings vary due to the fluctuation of energy costs. Hence, the investment is evaluated energetically. The energy saved with the efficiency increase is opposed to the energy consumed by the application of the measure (energy investment). Energy is expressed in primary energy and in that way independent of any economic fluctuations. In addition, energy saving measures are investigated uncoupled from their cost-effectiveness and especially grants. Nevertheless, in industry cost evaluation will determine the decision.

Heat integration has turned out to be one of the most powerful measures for energy efficiency increase. Streams to be cooled (hot streams) transfer their excess heat to streams to be heated (cold streams) via an additional heat exchanger in order to save external utilities.

Pinch analysis, the most common systematic approach to heat integration, is well known and widely established in continuous processes. In batch processes, this procedure is rarely used due to the challenges of small heat amounts and only temporally existing hot and cold streams. Indeed, in

previous approaches the internally exchangeable heat could be determined, but only for streams with constant supply and target temperatures. When heating or cooling in a vessel, the temperatures of the heat release or supply vary over time. This progression can e.g. be approximated with a linear or an exponential function (see figure 1).

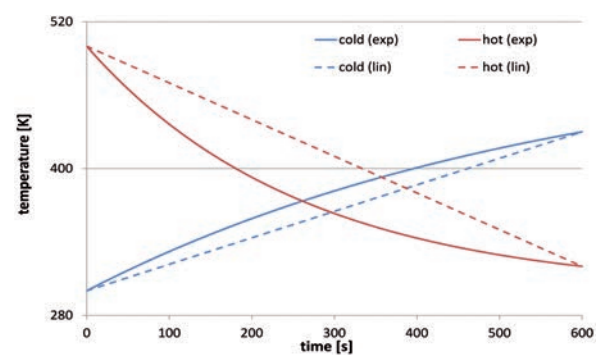


Figure 1: Depiction of streams with temperature progression.

In a new approach, streams with temperature progression are divided into time intervals so that the internally exchangeable heat can be determined exactly. The connection of the streams (matches) in these small time intervals leads to a huge number of small heat exchangers. Therefore, an evaluation matrix has been developed preferring those matches occurring in as many intervals as possible.

While temporally coexisting streams can be connected for direct heat exchange, heat storages have to be applied to integrate two streams, which do not exist at the same time. A guideline for the choice of an appropriate heat storage material was developed.

### Publications:

C. Dowidat, K. Ulonska, C. Bramsiepe, G. Schembecker  
 "Heat integration for batch processes with time dependent temperature profiles" ANQUE ICCE 2012 Sevilla (Poster)

### Contact:

Christian.Dowidat@bci.tu-dortmund.de  
 Christian.Bramsiepe@bci.tu-dortmund.de  
 Gerhard.Schembecker@bci.tu-dortmund.de

## Sequential model parameter determination procedure to simulate induced nucleation crystallization processes

Kerstin Wohlgemuth, Gerhard Schembecker

The control of batch crystallizations is difficult so that the prediction of crystal size distribution (CSD), as decisive quality criterion, at the end of the batch run is important. Out of specification products lead to high resource consumption and profit loss and should be avoided. The control of nucleation is essential, wherefore induced nucleation processes, such as sono- and gassing crystallizations, are focused on. A model is developed to simulate the crystal size distribution in dependence of process parameters, where a high number of model parameters have to be determined. Normally this is done by fitting them simultaneously to experimental data, which is time consuming. Therefore, a sequential parameter determination procedure is developed.

The reproducibility of batch crystallizations is challenging due to uncontrolled nucleation processes. Seeding is one strategy to control nucleation, but is more an art than a science. Alternatives are sono- and gassing crystallizations. For the latter case a systematic study using the model system of L-alanine/water and Design of Experiments was done investigating the impact of process parameters like initial supersaturation, gassing period and gas flow on the resulting CSD.

The model developed based on a population balance, which takes all important phenomena such as nucleation, crystal growth, agglomeration and breakage into account (see Figure 1). All these phenomena introduce model parameters, which have to be fit to experimental data. A reduction of model parameters is desired and achieved by decoupling the crystallization phenomena and fit the parameters sequentially.

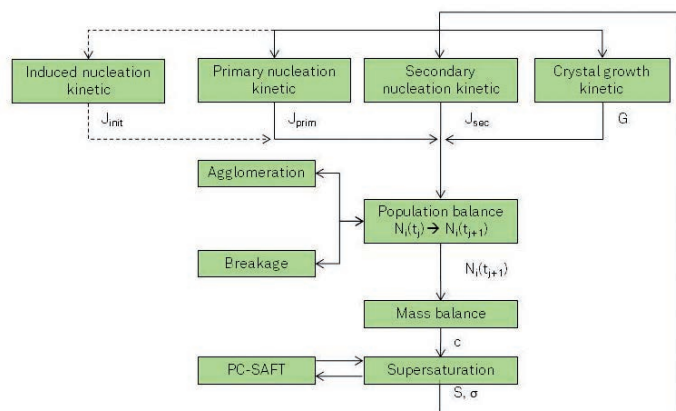


Figure 1: Model parameter determination procedure.

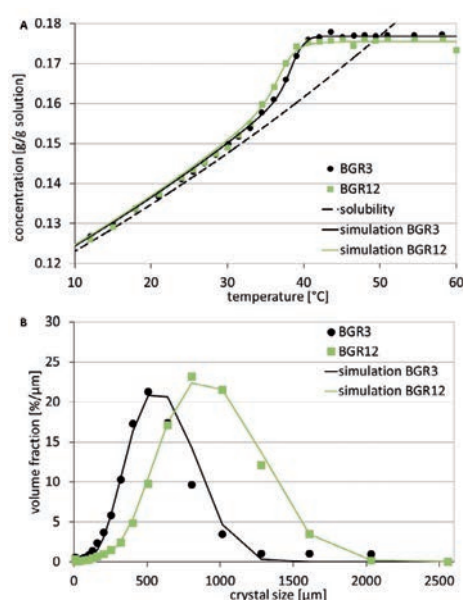


Figure 2: Simulation result of two gassing crystallizations of L-alanine/water.

Within this approach, first the nucleation parameter of primary nucleation is adjusted to the point of concentration decrease of experimental data. Afterwards the induced nucleation parameter is determined by reducing the value of the nucleation parameter until significant nucleation is induced. Third step is the adjustment of crystal growth parameters, fitting the whole concentration profile. If the profile cannot sufficiently be determined, secondary nucleation is added. In a last step CSD is adjusted using agglomeration, breakage or both parallel. To choose the right mechanism crystal images are checked first. Figure 2 shows two exemplary results of gassing crystallizations with different process parameters. With the aid of the parameter determination procedure developed the experimental data can be simulated well.

Contact:  
 Kerstin.Wohlgemuth@bci.tu-dortmund.de  
 Gerhard.Schembecker@bci.tu-dortmund.de

#### Publications:

- Kordylla, A.; Krawczyk, T.; Tumakaka, F.; Schembecker, G. (2009): Modeling Ultrasound-induced Nucleation during Cooling Crystallization. In: Chemical Engineering Science 64 (8), p. 1635–1642.
- Wohlgemuth, K.; Kordylla, A.; Ruether, F.; Schembecker, G. (2009): Experimental study of the effect of bubbles on nucleation during batch cooling crystallization. In: Chemical Engineering Science 64, p. 4155–4163.
- Wohlgemuth, K.; Ruether, F.; Schembecker, G. (2010): Sonocrystallization and Crystallization with Gassing of Adipic Acid. In: Chemical Engineering Science 65 (2), p. 1016–1027.
- Schembecker, G.; Ruether, F.; Wohlgemuth, K. (2011): Induced nucleation processes. ICMAT, Singapore, Singapore.
- Wohlgemuth, K.; Schembecker, G. (2011): On the way understanding induced nucleation processes using it for process design. ISIC 18, Zurich, Switzerland.





## Biomaterials and Polymer Science (BMP)

## Stress-induced melting of crystals in natural rubber

*A new way to tailor the transition temperature of shape memory polymers*

Benjamin Heuwers, Dominik Quitmann, Frank Katzenberg, Jörg C. Tiller

Lightly cross-linked natural rubber (NR, *cis*-1,4-polyisoprene) was found to be an exceptional cold programmable shape memory polymer (SMP) with strain storage of up to 1000 %. These networks are stabilized by strain-induced crystals. We found that the material recovers its original shape at a critical stress transverse to the strain-stabilized direction. It could be shown that this is due to disruption of the strain-stabilizing crystals, which represents a completely new trigger for SMPs. The variation of transverse stress allows tuning of the trigger temperature  $T_{\text{trig}}(\sigma)$  in a range of 45 °C to 0 °C, which is the first example of manipulating the transition of a crystal-stabilized SMP after programming.

In this study, we explored the influence of external stress perpendicular to the stretching direction during programming (referred to as transverse stress  $\sigma_t$ ) on the melting temperature of crystals in elongation-stabilized natural rubber.

Therefore, NR samples were programmed to gain the temporary state of retained elongation using three different stretching temperatures of 30 °C (NR1), 45 °C (NR2) and 60 °C (NR3) which result in average trigger temperatures of the externally unstressed samples of  $T_{\text{trig,NR1}} = 25.8$  °C,  $T_{\text{trig,NR2}} = 30.5$  °C and  $T_{\text{trig,NR3}} = 38.4$  °C. These samples were cooled, loaded with different stresses transverse to strain-stabilizing direction and slowly heated up until the permanent shape recovered. Additionally, the sample NR2 was loaded with a stress rate at different constant temperatures until the permanent shape recovered upon certain trigger stresses  $\sigma_{\text{trig}}$ .

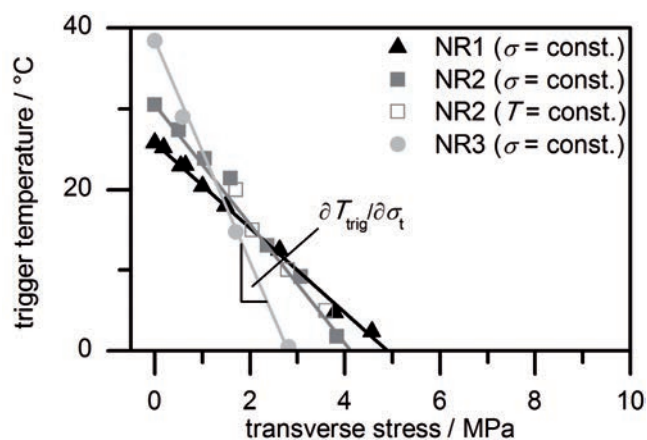


**Figure 1:** Plot of trigger temperatures of NR1, NR2 and NR3 versus applied transverse stress. Filled symbols correspond to values obtained by increasing temperature while keeping stress constant and open symbols to values obtained by increasing stress while keeping temperature constant.

The determined trigger temperatures are plotted versus the applied stress to compare the decrease of trigger temperature  $T_{\text{trig}}(\sigma_t)$  by transverse stress  $\sigma_t$  (**Figure 1**). The curve progression of all samples show linear trends of  $T_{\text{trig}}(\sigma_t)$  on  $\sigma_t$  but the lines of NR1, NR2 and NR3 cross each other. This indicates that NR samples tuned to a higher unstressed trigger temperature are more sensitive to transverse stress than those tuned to a lower trigger temperature.

In conclusion, if a programmed natural rubber shape memory polymer is loaded with stress transverse to the strain-stabilizing direction the original shape recovers upon a certain trigger stress  $\sigma_{\text{trig}}$  very sharply without external heat supply. This effect is due to a linear decrease of the original trigger temperature upon mechanical stress, followed by crystal disruption. Thus, we define such a stress-induced disruption of the strain-stabilizing crystals as stress-induced melting (SIM). This opportunity of stress-induced melting of the elongation stabilizing crystals without the need of any additional heat offers a completely new trigger to release stored strain of crystal-stabilized shape memory polymers. Additionally, the variation of transverse stress allows tuning of the trigger temperature  $T_{\text{trig}}(\sigma)$  in a range of 45 °C to 0 °C after programming. Further, the material might be used as a force actuator (stress sensing and overload protection) due to a critical trigger stress  $\sigma_{\text{trig}}$ . Moreover, the application of different programming temperatures and transverse stresses allows two-dimensional tuning of the trigger temperature and makes this shape memory polymer unique. Interestingly, the individual stress sensitivity  $\Delta T_{\text{trig}}/\Delta \sigma_t$  can be adjusted by the programming procedure.

**Contact:**  
benjamin.heuwers@udo.edu  
dominik.quitmann@udo.edu  
frank.katzenberg@udo.edu  
joerg.tiller@udo.edu

Publications:  
B. Heuwers, D. Quitmann, F. Katzenberg, J. C. Tiller, *Macromolecular Rapid Communications* 2012, accepted, DOI: 10.1002/marc.201200313  
F. Katzenberg, B. Heuwers, J.C. Tiller, *Advanced Materials* 2011, 23, 1909–1911

## Polymer Enzyme conjugates with Poly(oxazoline)s

### Organosoluble enzyme conjugates for biocatalysis

Stefan Konieczny and Jörg C. Tiller

Enzymes can be used as selective and highly active biocatalysts for the synthesis of complex organic compounds. By the usage of enzymes in organic solvents, their potential can be greatly extended and this is therefore in focus of current research. Here we report the synthesis of fully organosoluble poly(2-oxazoline) (POx) enzyme conjugates with different enzymes using a new coupling technique.

One way for the application of enzymes in organic media is the chemical modification with polymers. Through such a modification, the enzymes become soluble in the organic solvent and this leads to a higher catalytic activity.

The POXylation was carried out reacting pyromellitic acid dianhydride (PADA) as bifunctional reagent subsequently with ethylenediamine terminated POx and then with the NH<sub>2</sub>-groups of the respective enzymes.

It could be shown, that the PADA can be used to modify the polymers and use the derivatives without further modification.

Upon conjugation with the polymers, RNase A and lysozyme became fully soluble in DMF (1.4 mg/ml). These are the first examples of fully POXylated proteins, which become organosoluble (Fig. 1).



**Figure 1:** From left to right ~7 mg lysozyme in 5 ml DMF: native; modified with PADA (5.0 mg) only; modified with poly(2-methyl-1,3-oxazoline) (81.3 mg) and PADA (5.0 mg).

The synthesized enzyme conjugates were characterized by SDS-PAGE, isoelectric focusing, dynamic light scattering and size exclusion chromatography, which all indicated the full POXylation of the enzymes (Fig. 2).

Interestingly, the degree of modification as well as the nature of the modified proteins is controlling the formation of aggregates in solution.

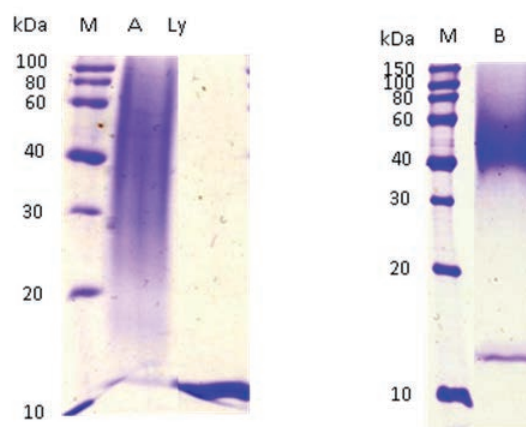


**Figure 2:** SDS-PAGE of lysozyme and the corresponding POx enzyme conjugates modified in DMF: (left) M Marker; Ly, lysozyme; A, lysozyme modified with poly(2-methyl-1,3-oxazoline); (right) B, lysozyme modified with poly(2-ethyl-1,3-oxazoline).

The modified lysozyme and  $\alpha$ -chymotrypsin even partly retained their activity in water and in the case of lipases also in chloroform.

It could be demonstrated with  $\alpha$ -chymotrypsin as example, that the molecular weight of the attached polymer significantly influences the activity in water depending on the size of the substrate.

In current and future experiments the solubility and enzymatic activity of the conjugates in other organic solvents will be tested.

By the usage of other POx and/or altering the modification parameters it might be possible to achieve solubility in other organic solvents as well. The developed strategy for the synthesis of polymer enzyme conjugates can also be used for further enzymes.

#### Publications:

Stefan Konieczny, Christoph P. Fik, Nils J.H. Aversch, Joerg C. Tiller Organosoluble enzyme conjugates with poly(2-oxazoline)s via pyromellitic acid dianhydride, *J. Biotechnol.* 159 (2012) 195–203

#### Contact:

stefan.konieczny@udo.edu  
joerg.tiller@udo.edu

## Amphiphilic Poly(2-oxazoline) ABA-Triblock Copolymers

*Building highly form-stable defined polymersomes*

Christian Krumm, Christoph P. Fik, Monika Meuris, Georg J. Dropalla, Helma Geltenpoth, Albert Sickmann, Jörg C. Tiller

*The formation of well-defined supramolecular structures is the key to future materials. We demonstrate that water-soluble ABA triblock copolymers based on poly(2-oxazolines) are capable of forming form-stable polymersomes in aqueous solution without using nano precipitation techniques. These structures coexist with micellar and unimicellar motives as shown with dynamic light scattering and electron microscopy.*

Self-organization of block copolymers in solution is a way to obtain advanced functional superstructures. The synthesis of well-defined polymethyloxazoline-*block*-polyphenyloxazoline-*block*-polymethyloxazoline (PMOx-*b*-PPhOx-*b*-PMOx) triblock copolymers is described and proven by  $^1\text{H}$  NMR spectroscopy, SEC and ESI-MS. The surprisingly water-soluble block copolymers did self-organize in aqueous solutions uniquely forming three coexisting well-defined structures: unimolecular micelles, micellar aggregates and very form-stable polymersomes. This is the first example of a polymersome forming ABA triblock copolymer with a glassy middle block. The spherical vesicles were analysed by electron microscopy. It could be shown that these vesicles are indeed hollow spheres.

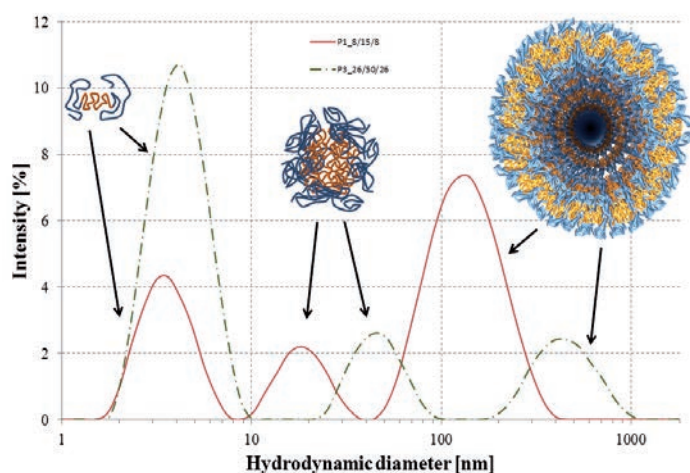


**Figure 1:** Hydrodynamic diameters vs. intensity plot of aqueous solutions of polymer (P1) and polymer (P3) respectively, measured by dynamic light scattering.

The preparation of PMOx-*b*-PPhOx-*b*-PMOx ABA triblock copolymers with defined block ratios and full control over the end-groups was successfully realized via cationic ring opening polymerization initiated by the commercially

available bifunctional  $\alpha, \alpha'$ -dibromo-*p*-xylene. The polymer with a 1:1 ration of the hydrophilic and the hydrophobic part formed three coexisting aggregates in their aqueous solutions (Fig. 1). This is one of the few examples, where defined polymersomes formed in water are stable enough to resist air-drying and can be imaged by electron microscopy (Fig. 2). We presume that this is due to the glassy PPhOx block in the middle of the ABA triblock copolymers.

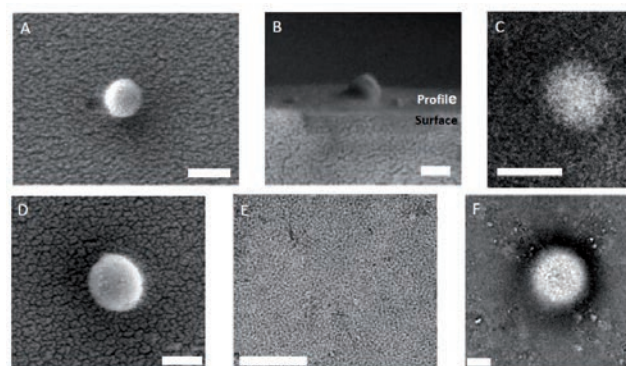


**Figure 2:** Scanning electron microscopy (SEM) images (A, B, D, E) of PMOx-*b*-PPhOx-*b*-PMOx triblock copolymer vesicles (P1: A, B) (P3: D, E). Transmission electron microscopy (TEM) image of PMOx-*b*-PPhOx-*b*-PMOx triblock copolymer vesicles (P1: C unstained) (P3: F stained with ruthenium tetroxide). 3E shows a TEM-image of stained polymeric matrix formed of the ABA triblock copolymer P3. All scale bars: 200 nm.

Currently, we investigate, if the polymersome formation can be influenced by different solvents, temperature or by the end groups particularly with respect to higher yield of the polymersomes. Preliminary studies have already shown that the solubility of the ABA triblock copolymers are greatly influenced by the end groups, e.g. ester functions render them water-insoluble. Further, we currently explore the possibility of entrapping functional molecules such as enzymes into the polymersomes and strive to find a functional initiator to crosslink the formed polymersomes.

Publications:  
Christian Krumm, Christoph P. Fik, Monika Meuris, Georg J. Dropalla, Helma Geltenpoth, Albert Sickmann, Joerg C. Tiller Well-Defined Amphiphilic Poly(2-oxazoline) ABA triblock Copolymers and Their Aggregation Behavior in Aqueous Solution, *Macromol. Rapid Commun.* 2012, DOI: 10.1002/marc.201200192

## Biocidal Polymers with Satellite Groups

### Influence of functional satellite groups on antimicrobial activity and hemotoxicity

Christoph P. Fik, Christian Krumm, Jörg C. Tiller

Antimicrobial polymers are considered as alternative to environmentally problematic biocides, disinfectants and even to antibiotics. It was found recently, that poly(2-oxazoline)s with an antimicrobial end group are also antimicrobially active. Most remarkably, their antimicrobial activity is controlled by the group distal to the biocidal function. Due to a new synthesis strategy, we were able to introduce functional satellite groups. These satellite groups also control the antimicrobial activity and even the hemotoxicity of the polymers.

Polyoxazolines with a biocidal quaternary ammonium end-group are potent biocides. The activity-controlling satellite groups had to be introduced via the initiator, and thus were non-functional, such as alkyl chains. The synthesis of a new antimicrobial initiator DDA-X allowed great variety of new satellites. Here, we present a study with a series of poly(2-methyloxazoline)s with varying functional satellite groups introduced upon termination of the polymerization reaction.

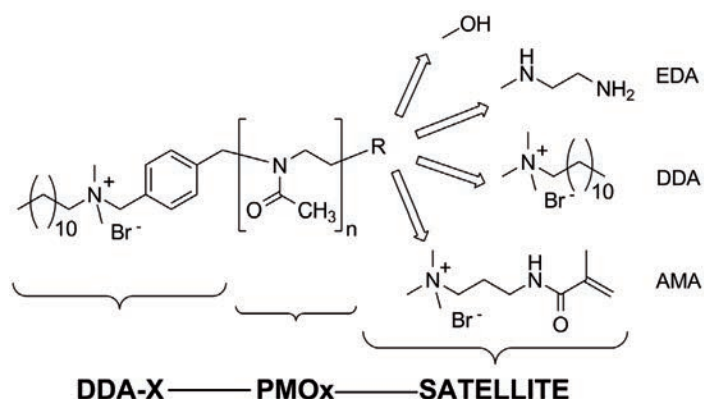


**Figure 1:** Telechelic poly(2-methyloxazoline)s (PMOx) with biocidal initiator (DDA-X) at the start position and varying functional satellites: (OH= hydroxyl, EDA= ethane-1,2-diamine, DDA= N,N-dimethyl-dodecylammonium bromide, AMA= 3-(methacryloyl-amino)-N,N-dimethylpropan-1-ammonium bromide) at the respective terminal position.

This allowed introducing a series of functional satellites, including hydroxy, primary amino, and double bond containing groups. The resulting telechelic poly(2-oxazoline)s were explored

regarding their antimicrobial activity and hemotoxicity. It was found that the functional satellite groups greatly controlled the minimal inhibitory concentrations against the bacteria *Staphylococcus aureus* and *Escherichia coli* in a range of 10 to 2500 ppm. Surprisingly, the satellite groups also controlled the hemotoxicity, but in a different way than the antimicrobial efficiency.

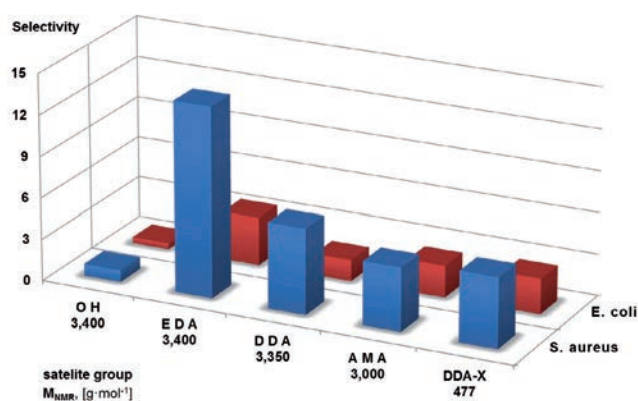


**Figure 2:** Selectivity values of the telechelic polymethyloxazolines DDA-X-PMOx-SATELLITE with varying satellite groups (=OH, EDA, DDA, AMA) in comparison to the biocidal low molecular weight initiator DDA-X. Calculated from HC50•MIC-1 ratios for each, *S. aureus* and *E. coli*.

It could be demonstrated that the introduction of one antimicrobial group (DDA-X) and one hydrophilic cationic satellite group (EDA) results in a highly active antimicrobial, less hemotoxic polymer, because both groups combine their different functions, membrane penetration and surface attraction, symbiotically in one polymer. Obviously, this kind of satellite groups might be useful for targeting multiple biological functions.

#### Publications:

C.P. Fik, C. Krumm, C. Münnig, T.I. Baur, U. Salz, T. Bock, J.C. Tiller  
Impact of Functional Satellite Groups on the Antimicrobial Activity and Hemocompatibility of Telechelic Poly(2-methyloxazoline)s  
*Biomacromolecules* 13 (1), 165-172 (2012)

#### Contact:

christoph.fik@udo.edu  
christian.krumm@udo.edu  
joerg.tiller@udo.edu

## APCN for activating enzymes in organic solvents

*Poly(2-oxazoline)-based APCN take up enzymes during preparation*

Stephan Dech, Jörg C. Tiller

The high functionality of modern materials is often achieved by a controlled nanostructure. Amphiphilic polymer conetworks (APCN) show such a nanostructure, which can be used to greatly activate entrapped enzymes in organic solvents. Unfortunately, the loading capacity and enzyme size are limited to less than 1 wt% loading and small enzymes. Here, we present a new APCN class that can be prepared in aqueous solutions and is capable of entrapping enzymes of any size with up to 11 wt.% loading. It was shown on the example of lipase that the entrapped enzymes are even higher activated in organic solvents than that in conventional APCNs.

Amphiphilic polymer conetworks represent a class of nanomaterials with great application potential, because they can combine the properties of two chemically different, immiscible polymers in one macroscopically homogeneous nanophasic material. Both polymer nanophases can act independently from each other. This is due to the fact that the conetworks consist of two polymers one crosslinked by the other, i.e. they are segmented conetworks. The copolymerization of Poly(2-ethyloxazoline) (PEtOx) macromonomers with 2-hydroxyethylacrylate (HEA) results in optically clear, homogeneous conetwork membranes (Fig. 1). DSC, DMA, and AFM measurements revealed that the membranes consist of two partially mixed polymer nanophases, which showed characteristic properties of amphiphilic conetworks (Fig. 2).



**Figure 1:** Photos of PHEA-*l*-PEtOx<sub>4.8</sub> conetwork in dried and water swollen state.

Lipase from *rhizomucor miehei* was successfully entrapped prior to the polymerization step for first time in those kinds of conetworks. The high activity of immobilized RmL in water indicates the efficiency of this mild method to entrap enzymes. The activity results for such captured RmL in organic solvents showed the superior properties of these new PHEA-*l*-PEtOx conetworks. Compared to the literature known PHEA-*l*-PDMS systems, an up to 6-fold higher specific activity and an up to 8-fold higher conetwork activity were obtained.

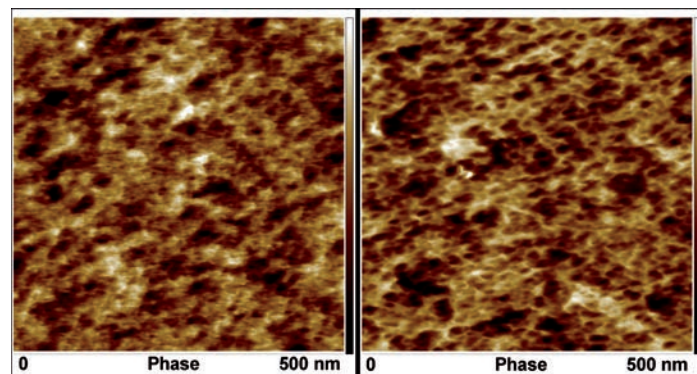


**Figure 2:** AFM images of PHEA-*l*-PEtOx<sub>4.8</sub> conetworks with 50 and 70 wt.% PEtOx<sub>4.8</sub> (from left to right). Images were recorded in tapping, phase mode. Phase contrast here is 8° (left) and 21° (right).

This makes PHEA-*l*-PEtOx conetworks outstanding materials for enzyme entrapment and their use as nanoreactors for biocatalytic reactions in organic media. Also numerous other larger functional structures such as nanoparticles, antibodies or even ion pumps might be entrapped into such conetworks.

Publications:  
S. Dech, V. Wruk, C.P. Fik, J.C. Tiller  
Amphiphilic Polymer Conetworks Derived from Aqueous Solutions for Biocatalysis in Organic Solvents. *Polymer* 53, 701-707 (2012)



## Chemical Biotechnology (BT)

## Anaerobic Carbon Oxyfunctionalization

### *In vivo* coupling of nitrate reduction and quinoline hydroxylation in recombinant *Pseudomonas*

F. Özde Ütkür, Bruno Bühler and Andreas Schmid

Molybdenum (Mo) hydroxylases are interesting enzymes for industrial applications, as they derive the oxygen atom for substrate hydroxylation from water, thereby depending on an electron acceptor. This suggests that whole cells containing Mo hydroxylases may be used as biocatalysts for carbon oxyfunctionalizations in alternative respiratory systems, where electrons generated during substrate hydroxylation are directed to an inorganic electron acceptor such as nitrate, rather than molecular oxygen. Here, we show the capability of whole cells containing a Mo hydroxylase to achieve anaerobic carbon oxyfunctionalization as a proof of concept, which, in future, may result in a reduced oxygen demand in technical applications.

With whole cells containing Mo hydroxylases, molecular oxygen is not required for substrate hydroxylation, but only as the respiration substrate. In alternative respiratory systems, Mo enzymes may be applied by coupling oxyfunctionalization to inorganic substrate reduction. In order to evaluate the suitability of whole-cell biocatalysts based on Mo hydroxylases in alternative respiratory systems, quinoline 2-oxidoreductase (Qor)-containing *Pseudomonas putida* 86 was tested for quinoline hydroxylation coupled to denitrification under anoxic conditions (Fig. 1). It is important to note that, under anoxic conditions, 2-hydroxyquinoline is expected to be the sole product, whereas, under oxic conditions, further metabolism in the coumarin pathway occurs via oxygenation.

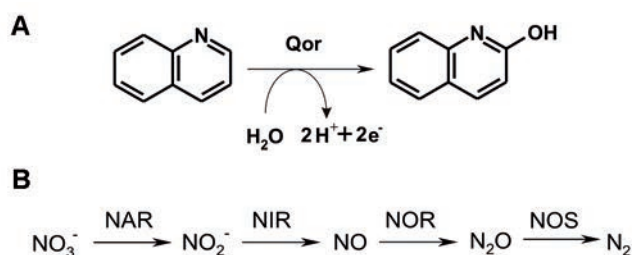
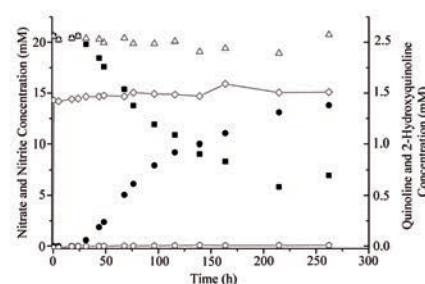


**Figure 1:** Coupling of oxyfunctionalization to inorganic substrate reduction. A. First step in the coumarin pathway of quinoline degradation. Quinoline 2-oxidoreductase hydroxylates quinoline in *ortho* position to 2-hydroxyquinoline, introducing the oxygen atom from water. B. Denitrification pathway in *Pseudomonas aeruginosa*. Nitrate, nitrite, nitric oxide, and nitrous oxide reductases are depicted as NAR, NIR, NOR, and NOS, respectively.

*P. putida* 86 was found to be capable of reducing both nitrate and nitrite, but at rather low rates and without the ability to catalyse concomitant quinoline hydroxylation (Fig. 2A). To enhance the denitrification capacity of *P. putida* 86 and thus to enable quinoline hydroxylation, the denitrification genes coding for the nitrate reductase (NAR) from *P. aeruginosa* were introduced into *P. putida* 86. This

resulted in a Qor activity of 6.9 U g<sub>CDW</sub><sup>-1</sup> with recombinant *P. putida* 86 cells under anoxic conditions (Fig. 2B), which corresponds to 12.5% of the Qor activity of *P. putida* 86 under oxic conditions (~55 U g<sub>CDW</sub><sup>-1</sup>).

**A**



**B**

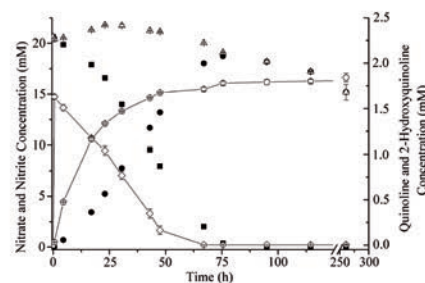


**Figure 2:** Depletion of nitrate (■) and quinoline (◇) and formation of nitrite (●) and 2-hydroxyquinoline (△) by A. *P. putida* 86 (pLAFR3) and B. *P. putida* 86 (pNQ07) (at a cell concentration of 0.3 g<sub>CDW</sub> l<sup>-1</sup>). (Δ) depicts the total concentration of nitrate and nitrite.

To conclude, the feasibility of anoxic substrate hydroxylation using Mo hydroxylases has been shown as a proof of concept and remains to be evaluated in a process set-up. For the development of a productive technical application, the denitrifying capacity of *P. putida* may be enhanced by the functional expression of all genes involved in denitrification (Fig. 1B).

**Contact:**

oezde.uetkuer@bci.tu-dortmund.de  
andreas.schmid@bci.tu-dortmund.de  
bruno.buehler@bci.tu-dortmund.de

## Towards a constitutive solvent tolerant phenotype of *Pseudomonas* sp. strain VLB120

Jan Volmer, Bruno Bühler and Andreas Schmid

Up to now, *E. coli* strains are mostly applied for whole-cell oxygenase-based redox biocatalysis due to their well-studied characteristics and the ease of handling with respect to growth and genetic manipulation. However, in the case of redox biocatalysis with toxic reactants, *Pseudomonas* strains are a promising alternative due to their solvent tolerance and high metabolic versatility and capacity. Here, solvent tolerance mechanisms of *Pseudomonas* strain VLB120 were investigated and a constitutive solvent tolerant strain was constructed by means of genetic engineering.

The use of whole cells as biocatalysts is often limited due to the presence of organic compounds, either as substrates or (side) products, which are toxic to living microorganisms. The toxic effect is usually based on the intercalation of the organic substances into the cell membrane, thus increasing membrane fluidity and permeability, which disturbs cellular homeostasis and finally leads to cell death.

One promising approach to overcome limitation by toxic organic compounds is the use of solvent tolerant microorganisms, such as *Pseudomonas* strains, which are able to tolerate high amounts of toxic solvents due to several adaptive mechanisms. The main mechanism counteracting solvent toxicity is the energy-dependent efflux of organic compounds via membrane pumps. As these solvent efflux pumps act as a long term response, *Pseudomonas* strains need to be adapted to develop a solvent tolerant phenotype. Typically, these adaptation procedures are unpredictable and tedious. Furthermore, solvent tolerance is lost fast after switching to solvent free conditions.

By genome analysis of *Pseudomonas* sp. strain VLB120, genes involved in solvent tolerance were identified with the solvent efflux pump TtgGHI as a main factor counteracting solvent toxicity. To avoid long adaptation procedures, the repressor gene *ttgV* of this efflux pump was knocked out (Fig. 1),

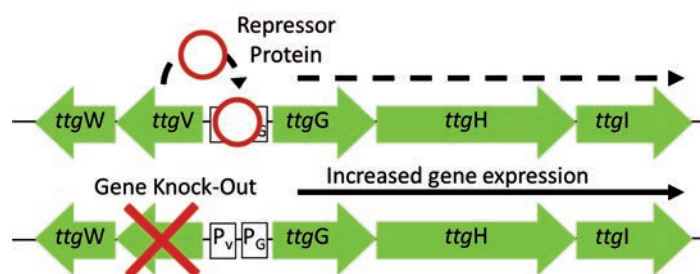


**Figure 1:** Solvent efflux pump gene cluster of *Pseudomonas* sp. strain VLB120. The repressor gene *ttgV* was deleted by homologous recombination with *ttgV::Km* and excision of the antibiotic cassette using the *Cre/loxP* system.

This *Pseudomonas* VLB120 $\Delta$ *ttgV* mutant showed tolerance towards highly toxic toluene without the need for adaptation, while the wildtype strain *Pseudomonas* VLB120 showed a 20 h lag phase (Fig. 2). The final biomass titer reached was the same for both strains.

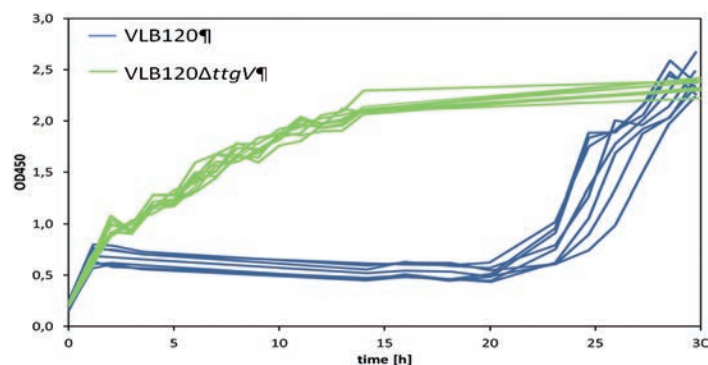


**Figure 2:** Growth of *Pseudomonas* sp. strain VLB120 and VLB120 $\Delta$ *ttgV* on LB medium in the presence of 1% (v/v) toluene. Toluene was added after 1 h of cultivation.

This constitutive solvent tolerant strain is an excellent starting point for the further development of *Pseudomonas* to a whole-cell redox biocatalysis platform in toxic environments.

Oral presentation:  
Volmer J., Bühler B. and Schmid A., Towards a stable solvent tolerant phenotype of *Pseudomonas* sp. strain VLB120 for redox biocatalysis with toxic reactants, CLIB Graduate Cluster Annual Retreat 2012, Bergisch Gladbach

Contact:  
jan.volmer@bci.tu-dortmund.de  
bruno.buehler@bci.tu-dortmund.de  
andreas.schmid@bci.tu-dortmund.de

## Improved proline 4-hydroxylase (P4H) by random mutagenesis

*Protein engineering as a procedure for enzyme optimization*

Jianan Fu, Katja Bühler and Andreas Schmid

Oxygenases like P4H are highly interesting for the chemical and pharmaceutical industry because of their ability to introduce oxygen into C-H bonds with high stereoselectivity [Antioxid Redox Signal (2010)13:349-94]. The development of novel powerful enzyme design tools and screening methods allowed for optimizing or creating enzymes with better features for industrial applications. In this work, a proline 4-hydroxylase (P4H) mutagenesis library was generated by sequence saturation mutagenesis, using the wild type P4H1 from *Dactylosporangium sp. RH1* [Appl Environ Microbiol (1999) 65(9): 4028-31] as a template.

P4H, an  $\alpha$ -ketoglutarate dependent dioxygenase (aKGDO), was first described in the 1980's from *Streptomyces griseoviridus* P8648 [Biochem Biophys Res Commun (1984) 120:45]. The interest in this enzyme family has increased significantly in the recent years, as many of these enzymes are located in pathways which are of medical or pharmaceutical significance [Nat Prod Rep (2000) 17:367].

A P4H mutagenesis library was generated by sequence saturation mutagenesis (SeSaM-Tv+) [Biotechnol J (2008) 3:74]. Medium throughput screening procedures were developed to identify mutagenesis variants with different *in vitro* as well as *in vivo* catalytic efficiency and performance.

For the screening procedure, cell growth and *p4h* gene expression were synchronized in a 96-well microtiter plate. A huge variety of P4H mutants was detected, showing different activities compared to the wild type enzyme *in vitro* and *in vivo* (Figure 1).

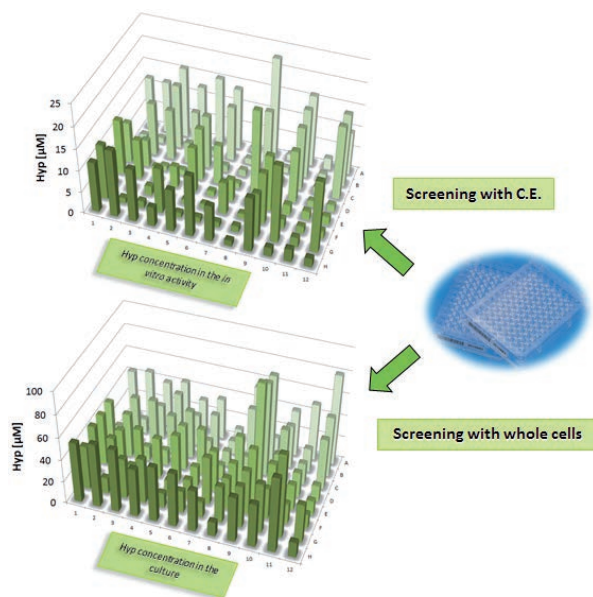


**Figure 1:** Screening of P4H mutants using either crude cell extract (CE; upper panel) or whole cells (lower panel). The assay detected the final product concentrations. For *in vitro* screening using crude cell extract, the cells were lysed after an overnight cultivation and subjected to an activity assay, while product concentration was directly measured in the supernatant of the culture during the *in vivo* screening using whole cells expressing mutated *p4h*.

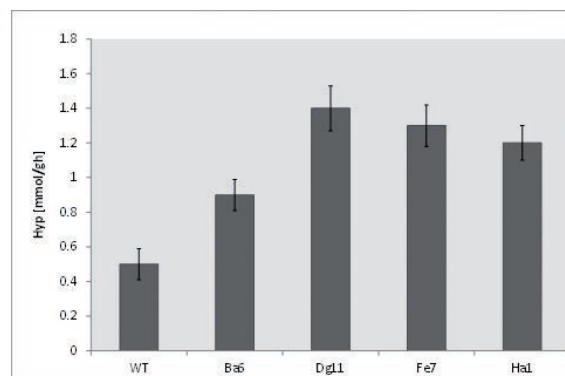


**Figure 2:** Four promising P4H mutants were chosen and investigated in shaking flasks. The mutant enzymes showed up to 3 fold higher hydroxyproline production rates and a 2-fold higher yield on proline in whole cells.

Surprisingly, in the crude cell extracts no mutants showing a higher catalytic activity than the wildtype enzyme could be identified, whereas a couple of interesting candidates with significant improved production rates and yields were detected in the whole cell supernatants (Figure 2). These results indicate that the mere biochemical characteristics of the respective enzymes are not the only parameters influencing the biocatalytic performance of a whole cell biocatalyst. Especially parameters like enzyme stability and reaction uncoupling may significantly influence whole-cell biocatalyst performance and will now be evaluated in detail for the respective P4H mutants.

## Segmented flow biofilm membrane microreactors

### Novel reactor for bioprocess intensification

Rohan Karande, Katja Buehler and Andreas Schmid

Biofilms are surface associated microbial communities embedded within a self-generated extracellular polymeric matrix (EPS) that are ubiquitous in natural environments. In the context of biocatalysis, biofilm forming microorganisms can circumvent classical pitfalls of planktonic cells like short term operational stability and solvent toxicity by its aptitude to self-immobilize and self-renewal in the EPS matrix. Additionally, biofilms can sustain five to ten fold higher biomass per unit volume compared to suspended cells, which should contribute to improved volumetric reaction rates. However, diffusion limitation of the substrates might offset this advantage by the reduced effectiveness of the biomass. We have developed a novel biofilm reactor, which is simple both in concept and execution, and exploits the potential of interacting the biofilm, the fluid mechanics phenomena, and the membrane to overcome mass transfer limitations.

Biofilm reactors very frequently involve multiple phases for the transfer of low soluble substrates (e.g., oxygen or organic substrates). Major challenges in the development of multiphasic biofilm reactors are sufficient oxygen supply, high interfacial mass transfer at low energy input and easy scale up.

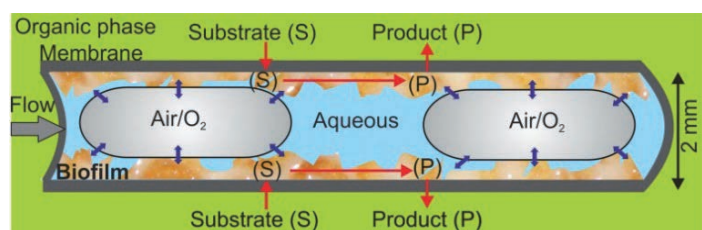


**Figure 1:** Schematic view of a two-phase (aqueous-air) segmented flow biofilm membrane microreactor (SFBMR). The organic substrate diffuses through the membrane into the biofilm where the product formed is extracted into the organic phase. Glucose and oxygen are supplied via alternating aqueous and air segments.

In the recent years, segmented or drop flow microreactors have been developed to an attractive platform for conducting multiphasic reactions because of excellent mass transfer performance between, and within the segments. This results from very high surface area to volume ratio and rapid mixing within the segments. In this work, the concept of segmented flow biofilm microreactors (SFBMR) was developed for continuous biocatalytic production of chemicals with an aim to combine the advantages of biofilms and of segmented flow in membrane microreactors (Figure 1).

As a proof of concept, the performance of SFBMR was evaluated for the asymmetric epoxidation of styrene to (S)-styrene oxide using *Pseudomonas* sp. VLB120ΔC as catalytic biofilm.

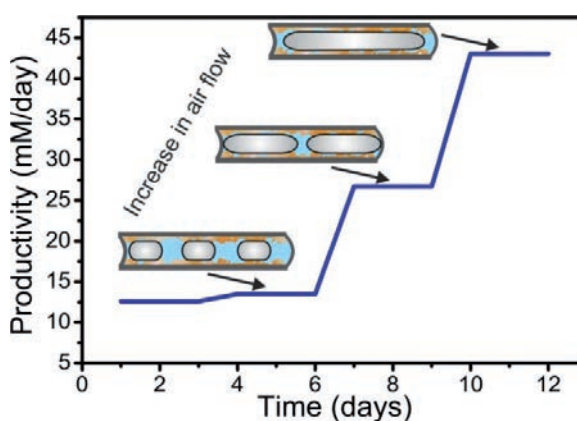


**Figure 2:** Improvement in styrene oxide volumetric productivity with increase in air flow rates in the SFBMR.

Varying the different phase flow rates significantly influenced the performance of the SFBMR (Figure 2). Increasing the air flow rate to an aqueous phase ratio of 16 and a dilution rate of 41 resulted in a maximal volumetric productivity of 42 mM styrene oxide / day (46 g/L tube volume/day).

Furthermore, the SFBMR was successfully applied to the biochemical hydroxylation of octane to *n*-octanol, using the biofilm forming strain *Pseudomonas putida* PpS81 pBT10. This work shows that SFBMR can be flexibly adapted to new biofilm reactions as a suitable platform technology.

#### Publications:

Schmid A., Karande R. and Buehler K. Segmented Flow Biofilm Reactor PCT/EP2011/057724, Patent filed (2011).  
 Karande R., Schmid A. and Buehler K. (2011) Miniaturizing Biocatalysis: Enzyme catalyzed reactions in an aqueous/organic segmented flow capillary microreactor. *Adv Syn Catal* 353:2511-2521

#### Contact:

katja.buehler@tu-dortmund.de  
 rohan.karande@tu-dortmund.de  
 andreas.schmid@tu-dortmund.de

## Single Cell Analysis with Picoliter nDEP Traps

### Single microbial cell analysis in controlled microenvironments

Oliver Frick, Frederik Fritsch, Christian Dusny and Andreas Schmid

Clonal microbial populations exhibit significant cell-to-cell differences, occurring on all hierarchical levels from genome to phenome, which cannot be revealed with conventional bulk measurement technologies. The extent of this physiological intrapopulation diversity was shown to correlate with frequency and strength of fluctuations in the extracellular environment. Development of the Envirostat 2.0 microfluidic chip enabled contactless cultivation of a single bacterial cell by negative dielectrophoresis (nDEP) in a precisely controllable microenvironment for the first time. Stable trapping in perfusing growth medium was achieved by a miniaturization of octupole electrode geometries, matching the dimensions of microbes. As a result, this leads to the ability to cultivate and analyze single cells in controlled microenvironments and hence to diminish physiological oscillations, posing a fundamental prerequisite for the disclosure of cellular functions beyond the population average. In this context we present a systematic investigation of microbial physiology at single cell level in controlled microenvironments employing the Envirostat 2.0 microfluidic single cell analysis system.

For the first time the Envirostat 2.0 allows contactless single bacterium isolation and trapping in controlled microenvironments (Fig. 1).

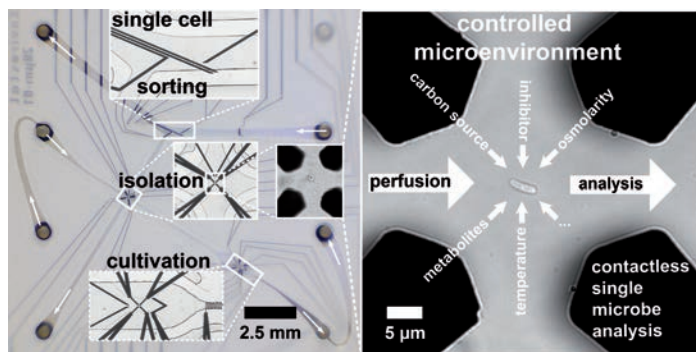


**Figure 1:** The ENVIROSTAT 2.0 enables precisely controlled microenvironments during contactless isolation and cultivation of singularized industrially relevant bacteria or other microbes in 1.7 pl nDEP traps.

The optimized microelectrode geometries and designed microfluidics enable: first, single (eu-) bacterium isolation from other cells to prevent cell-cell interactions, second, a fluid removal of preculture medium residues, and third, a precise microenvironmentally controlled nDEP trapping of a chosen microbe in a microchamber for single cell cultivation, perturbation, and analysis. Isolated cells in steady environments exhibited consistently faster volume growth rates that were up to 2-fold higher, as compared to cells cultivated and observed on population level (Fig. 2).

These results impressively constitute the Envirostat 2.0 single cell analysis system as an innovative and new flexible tool for elucidating cellular physiology at single cell level.

#### Contact:

oliver.frick@bci.tu-dortmund.de  
 frederik.fritsch@bci.tu-dortmund.de  
 christian.dusny@bci.tu-dortmund.de  
 andreas.schmid@bci.tu-dortmund.de

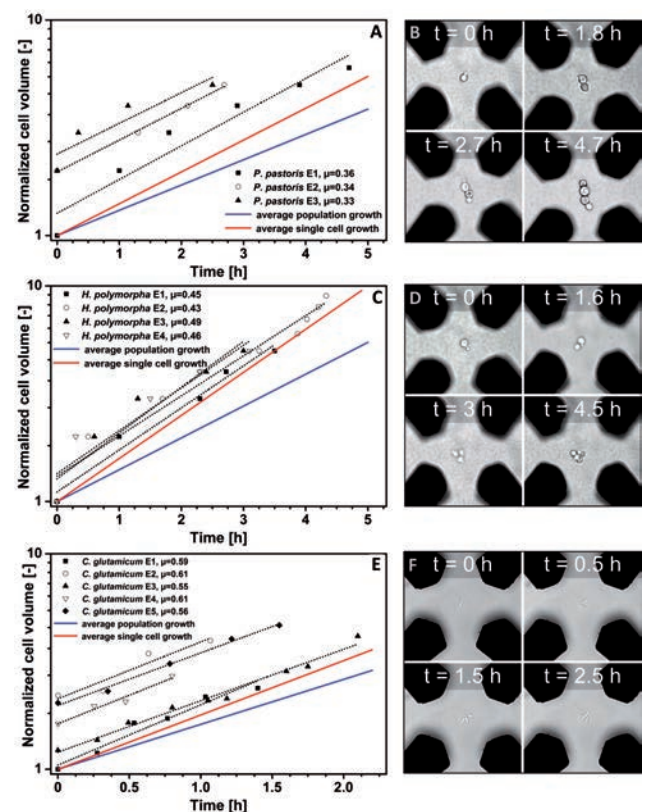


**Figure 2:** Volume growth analysis of single cells and micropopulations of industrially relevant eukaryotes and prokaryotes. The total cell volume of the trapped cells, normalized to the smallest observed cell within the respective series of experiments, is shown on the y axis in a common logarithmic scale. Red lines represent the average growth at single cell level; blue lines show the growth at population level.

#### Publications:

Fritsch F. S. O., Rosenthal K., Kampert A., Dusny C., Frick O., Blank L. M. and Schmid A., Picoliter nDEP traps enable time-resolved contactless single bacterial cell analysis in controlled microenvironments, Lab Chip, submitted (2012).  
 Dusny C., Fritsch F.S.O., Frick O. and Schmid A., Isolated Microbial Single Cells and Resulting Micropopulations Are Growing Faster in Controlled Environments, Appl. Environ. Microb., submitted (2012)  
 Fritsch F. S. O.\*, Dusny C.\*, Frick O. and Schmid A., Single Cell Analysis in Biotechnology, Systems Biology, and Biocatalysis., Ann. Rev. Chem. Biomol. Eng., accepted, (2012).



## Biochemical Engineering (BVT)

## Biopolymer immobilization of enzymes

### *Improving the immobilization efficiency in alginate microcapsules*

Markus Kampmann, Rolf Wichmann

*Biocatalysts are usually immobilized in order to protect them against deactivation and to facilitate their handling, separation and reutilisation. One option is the entrapment in biopolymer materials, e.g. alginates. Some advantages are the high biocompatibility and mild immobilization methods. However, when applied to immobilization of enzymes, leaching of biocatalysts from the biopolymer capsules is a fundamental challenge. We were able to obtain 80 % of the original enzyme activity in alginate microcapsules by use of different additives and self-designed experimental equipment. In another reaction the activity of immobilized enzyme was even higher than that of the native enzyme.*

The geometrical and rheological characteristics of biopolymer microcapsules are dependent on the polymer properties and the manufacturing process. For easier characterization of the enzyme carrier, highly spherical microcapsules with monomodal size distribution are favorable. In addition, to minimize mass transfer limitations and thereby enhance enzyme reaction rate, the surface area of the microcapsules should be increased.

These requirements have been met by the construction of an air jet nozzle, with which the capsules diameter can be adjusted without need for subsequent classifying.

Figure 1 shows alginate microcapsules with a diameter of about 400 µm and a sphericity near to 1, prepared with the designed nozzle.

In order to verify the suitability as an immobilization system, tyrosinase from *Agaricus bisporus* was chosen as a model enzyme and immobilized in different biopolymer

microcapsules.

By a targeted modification of the capsules material, i.e. combination of different polymers and additives, and evaluating enzyme loading, we were able to reduce enzyme leaching from alginate microcapsules and increase enzyme activity to a significant extent.

The comparison between native and immobilized tyrosinase with 3,4-Dihydroxy-L-phenylalanine as a substrate showed that 80 % of the used enzyme activity was retained in the microcapsules, despite the diffusion resistance of the polymer phase.

Moreover, when Bisphenol A was used as a substrate, the obtained reaction rate with immobilized tyrosinase was even higher than with native enzyme. This might be explained by a modification of the microenvironment of the enzyme, resulting in different reaction conditions, or reduction of inhibitory effects of substrate or product.

Since Bisphenol A is an endocrine disrupting substance found in different places in the environment, there is a great demand for its removal from e.g. wastewaters. Therefore the obtained results might be useful for wastewater treatment.

Promising results were also obtained with regard to enzyme activity and stability as well as reduction of catalyst costs by generation of tyrosinase containing single cells and cell debris from the mycelium of *A. bisporus* and subsequent immobilization.

The extension of this immobilization procedure to other enzyme systems and its application to low solubility or two-phase systems offers a great potential for process intensification.

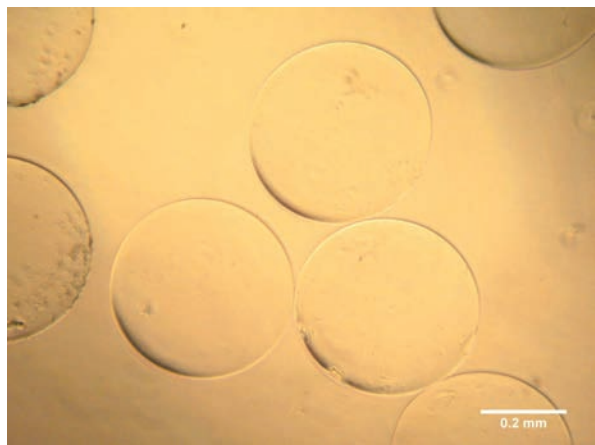


Figure 1: Alginate microcapsules. Scale bar represents 0.2 mm.

#### Contact:

markus.kampmann@bci.tu-dortmund.de  
rolf.wichmann@bci.tu-dortmund.de

#### Publications:

Kampmann, M., Kleiner, B., del Amor Villa, E.M., Wichmann, R., Enzyme encapsulation in Biopolymers, 8th European Congress of Chemical Engineering and 1st European Congress of Applied Biotechnology, Berlin, Germany (2011).

## Biobutanol Production

### Development of a continuous fermentation process

Mpho Setlhaku, Rolf Wichmann

The classical batch biological production of butanol from anaerobic fermentation of *Clostridium acetobutylicum* bacteria is governed by low total ABE (acetone, butanol, ethanol) solvent, low yield, low productivity and high butanol toxicity from 1%.

A two-stage process, where a continuous (first-stage) reactor coupled to a repeated fed-batch (second stage) has been developed. Two or more reactors are used alternatively in the second stage. The continuous reactor is kept at low butanol concentration, below toxicity and the second fed-batch stage is operated to result in the maximum products, 19.4 and 12 g l<sup>-1</sup> ABE and butanol respectively, Figure 1. This process is superior to batch and fed-batch fermentations, including two-stage continuous fermentation.

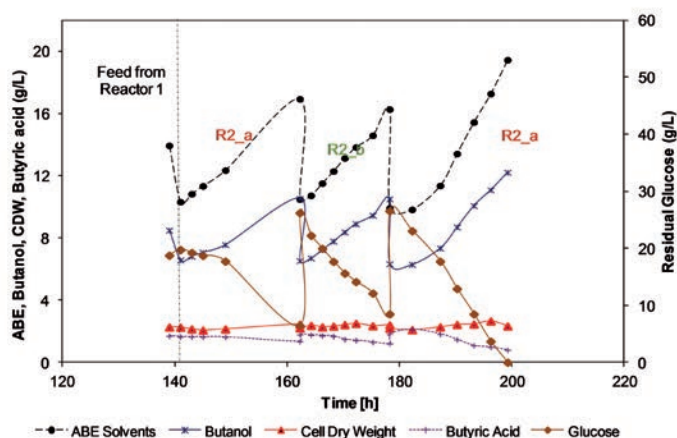


Figure 1: Overall ABE solvents, butanol, butyric acid, cell dry weight and glucose kinetics from two-stage fermentation operated continuously and in repeated fed-batch modes.

As butanol concentration of 12 g/L completely inhibits the growth of *C. acetobutylicum* cells. To alleviate butanol toxicity, gas stripping was investigated in one reactor setup operated continuously, Figure 2.

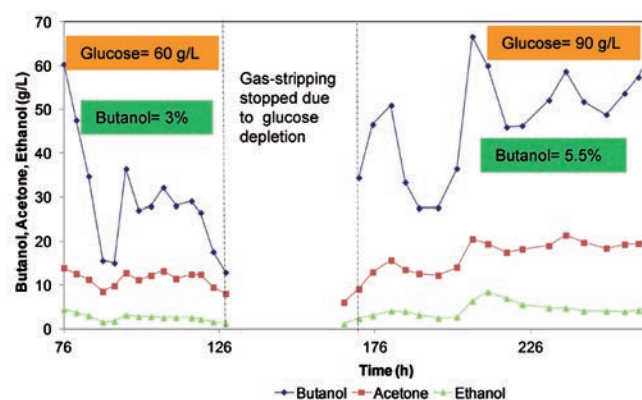


Figure 2: Butanol, acetone and ethanol in the condensate when gas-stripping is integrated into one-stage continuous fermenter.

During gas stripping butanol in the condensate could be concentrated up to 5.5% (w/v), Figure 2. Gas stripping made it possible to also increase glucose concentration in the medium, which resulted in the higher butanol in the condensate. Overall ABE productivity could be improved by 100%: gas stripping is now tested on the develop two-stage reactor ABE production process.

#### Publications:

Oral presentation: M.P. Setlhaku, E. M del Amor Villa, R. Wichmann, Biobutanol production using repeated batch with immobilized cell: process alternative to continuous, Bioengineering III, Lanzarote, Canary Islands (2011)  
Oral presentation: M.P. Setlhaku, E. M del Amor Villa, R. Wichmann, Repeated batch vs continuous fermentation for butanol production, RRB 7, Brugge, Belgium (2011)  
Oral presentation: M.P. Setlhaku, E. M del Amor Villa, R. Wichmann, Acetone-butanol-ethanol fermentation process improvement using continuous two-stage reactor with cell immobilization, ECAB-ECCE, Berlin, Germany (2011)  
Article: M. Setlhaku, S. Brunberg, E.M. del Amor Villa, R. Wichmann, Improvement in the bioreactor specific productivity by coupling continuous reactor with repeated fed-batch for acetone-butanol-ethanol production, J. Biotechnol. (2012), <http://dx.doi.org/10.1016/j.biotech.2012.04.004>

#### Contact:

mpho.setlhaku@bci.tu-dortmund.de  
rolf.wichmann@bci.tu-dortmund.de





## Process Dynamics and Operations (DYN)

## Realization of NMPC in an Industrial Polymerization Process

Tiago F. Finkler, Daniel Haßkerl and Sebastian Engell

In semi-batch polymerizations, it is usually desired to operate the system within a very tight temperature range and, at the same time, to feed the monomers into the reactor as fast as possible so that the batch durations are minimized. The simultaneous fulfillment of these both objectives implies that the system has to be operated very close to the limit of its cooling capacity, which requires efficient and reliable control. In this work, the operation of an industrial semi-batch polymerization reactor is optimized online using a NMPC (Nonlinear Model Predictive Control) scheme, as it is presented in Figure 1.

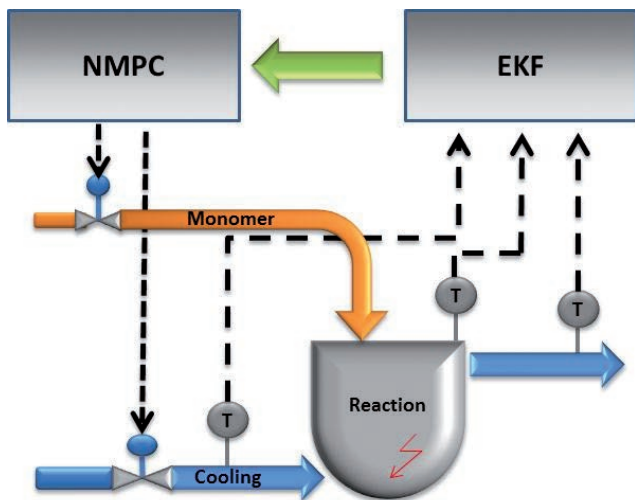


Figure 1: Scheme of the NMPC controller.

A semi-rigorous process model was developed in order to represent the real plant in simulations. It is based on a detailed description of the polymerization kinetics and it was used to check the robustness of the developed NMPC controller against several uncertainties in the operation scenarios, e.g. variations in the polymerization rate due to the formation of different active complexes, changes in the efficiency of the cooling system due to the generation of polymer during the batch and oscillations in the utilities supply. In addition, a simplified model was developed for the online optimization of the process operation. It can be simulated much faster than the complete model and it has correction factors for the reaction kinetics and for the heat transfer relations that can be updated online in order to compensate model uncertainties.

Since not all the relevant states of the reduced process model can be measured online, an EKF (Extended Kalman Filter) is used to reconstruct the state vector along the batch. Based on the temperature measurements, which are available every four seconds, the EKF provides online estimates of important unmeasured quantities like the rate of reaction, the heat transfer coefficient, the holdup of monomer and polymer in the reactor and the average molecular weight of the polymer.

Contact:  
tiago.finkler@bci.tu-dortmund.de

The NMPC controller was developed within a simulation environment that uses the complete semi-rigorous model to imitate the real process. After intensive investigations, important issues related to the practical implementation of the control scheme, e.g. development and validation of a reliable process model that can be used for online optimization during a batch, state estimation and online compensation of model uncertainties, were addressed. A preliminary version of the controller that controls only the reactor temperature was already tested at the real plant. The model predictive controller improved the quality of the temperature control significantly and was integrated within the DCS of the real process. In Figure 2, the performance of this model based controller is illustrated. Tests of the full NMPC controller with simultaneous temperature tracking and monomer feed maximization are planned for the near future.

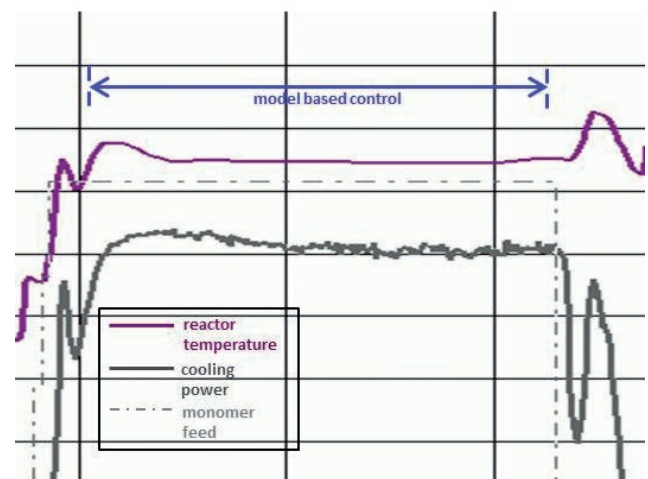


Figure 2: Test of the NMPC controller at the real plant.

Publications:  
T.F. Finkler, M. Kawohl, U. Piechottka and S. Engell (2012). Realization of Online Optimizing Control in an Industrial Polymerization Reactor. Keynote Lecture, IFAC Symposium on Advanced Control of Chemical Processes, Singapore.

## Timed Automata Based Scheduling for a Miniature Pipeless Plant with Mobile Robots

Christian Schoppmeyer, Martin Hufner, Subanatarajan Subbiah, Sebastian Engell

In contrast to traditional chemical plants, where the equipment is connected by pipes, pipeless plants use mobile production vessels to transport the materials between different processing stations. In our group, a miniaturized demonstration pipeless plant with autonomous guided vehicles (AGVs) that move the vessels between the stations has been realized. Planning and scheduling of multiproduct batch plants are challenging tasks that require support by intelligent decision-support systems in order to make sure that the scarce resources are utilized in an optimal fashion. In pipeless plants, in addition to the problem of distributing and sequencing the recipe operations on the available equipment, the problem of routing the mobile vessels in an efficient way must be addressed. We have modeled the scheduling problem in the miniature pipeless plant by timed automata (TA). The scheduling problem is then solved using reachability analysis. Two TA-based tools, TAOpt (developed in our group) and UPPAAL (developed by Uppsala University and Aalborg University) for computing schedules by reachability analysis were tested on the miniature pipeless plant example.

The miniature pipeless plant (Fig. 1), which was developed in the scope of the EU-project MULTIFORM, provides numerous design and control challenges on different levels of the control hierarchy. Here it is used as a benchmark problem for scheduling algorithms.

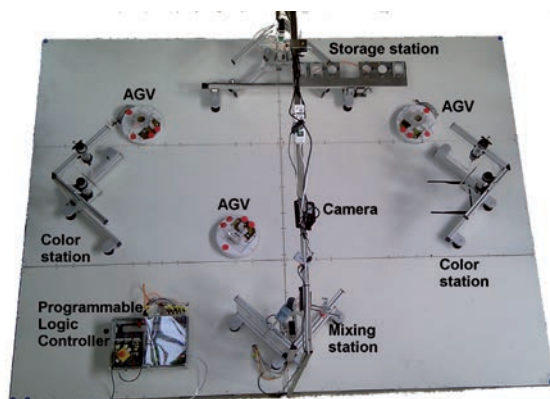


Figure 1: Picture of the miniature pipeless plant.

In our miniature pipeless plant, individually colored pieces of chalk are produced (see Fig. 2). The production of the pieces is performed in mobile vessels which are transported between the different processing stations by two AGVs. The plant consists of two filling stations which feed colored water to the vessels, one mixing station which adds plaster and mixes the compound, and one storage station which can store vessels that are either filled with material for hardening or empty.

The process steps for producing a piece of chalk are: an empty vessel from the storage station is transported to one or more filling station(s) and filled. The filled vessel is transported to a mixing station where plaster is added and mixed. The vessel is then transported to a storage station and left there for hardening in order to obtain a layer of the final product. Several cycles of this process can be executed to obtain multi-colored chalk sticks.



Figure 2: Pieces of crayon (boxed) with different layers.

The scheduling problem was modeled as a flexible job shop problem using TA (see Fig. 3) and solved using reachability analysis to obtain schedules that are then executed automatically.

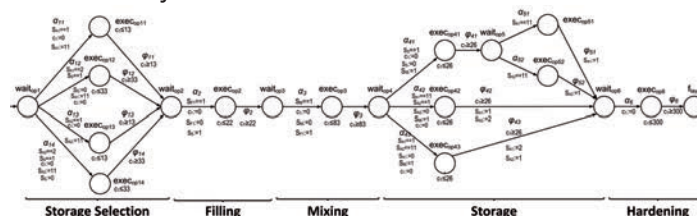


Figure 3: TA model of a complete recipe for one layer.

The comparative study showed that for obtaining feasible and good solutions fast, our TA-based scheduling tool TAOpt performs substantially better than UPPAAL.

Contact:  
 christian.schoppmeyer@bci.tu-dortmund.de  
 martin.huefner@bci.tu-dortmund.de  
 subanatarajan.subbiah@bci.tu-dortmund.de  
 sebastian.engell@bci.tu-dortmund.de

### Publications:

C. Schoppmeyer, M. Hufner, S. Subbiah, S. Engell: Timed Automata Based Scheduling for a Miniature Pipeless Plant with Mobile Robots. *Proc. IEEE Multi-Conference on Systems and Control*, Dubrovnik, October 2012.





## Fluid Separations (FVT)

## Membrane-Assisted Reactive Separation Processes

*An innovative tool for the selection and design of intensified processes*

Johannes Holtbrügge, Philip Lutze and Andrzej Górak

Due to decreasing fossil fuel reserves, the development of new and innovative processes leading to improvements in sustainability is necessary. Process intensification (PI) is considered to be one approach. Two outstanding examples within this group are the reactive and the membrane-assisted separation processes. Their combination promises even higher benefits compared to the single units. However, despite their advantages, these processes are not yet fully established in industry because the selection of suitable configurations and their design is difficult. Hence, to increase their application in industry, a tool for the selection and design of such processes is developed and validated for the production of dimethyl carbonate (DMC) and 1,2-propanediol from propylene carbonate and methanol (MeOH).

The design of a new process consists of three consecutive design steps. (1) Generation of different process alternatives, (2) evaluation and the choice of the best one and (3) final tuning of process parameters. Different process configurations are generated (1) performing a thermodynamic and chemical analysis of the investigated system. Due to the chemical equilibrium for this chemical system, the use of a reactive distillation (RD) is advisable. To overcome the thermodynamic equilibrium, especially azeotrope formation, a vapor permeation (VP) membrane is promising for the production of DMC.

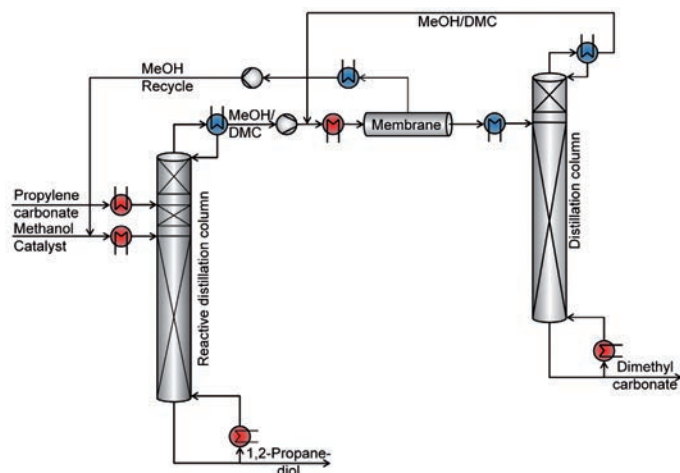


**Figure 1:** Simplified flowsheet of the membrane-assisted reactive separation process consisting of reactive distillation, vapor permeation and conventional distillation.

The evaluation (2) of different membrane-assisted reactive separation configurations comprising RD, VP and conventional distillation by a process analysis, using short-cut models, identified flowsheet 1 (Fig. 1) as the most promising and feasible configuration.

For the fine tuning of process parameters, detailed process models comprising a rate-based model for RD and an empirical solution-diffusion model for VP are developed. The parameters for the description of transmembrane

flux are determined in lab-scale permeation experiments using the hydrophilic membrane Sulzer Pervap™ 1255. To recycle unreacted MeOH to the RD, the selectivity towards MeOH is an important membrane property. Fig. 2 shows its temperature dependency at constant feed conditions.

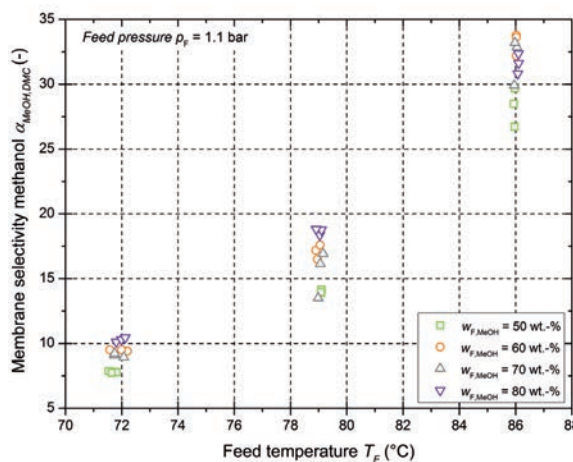


**Figure 2:** Experimental results of the temperature dependence of the membrane selectivity towards methanol in a binary mixture with dimethyl carbonate.

For the optimization problem (3) an evolutionary algorithm based on the “modified differential evolution” approach is used. This algorithm allows the simultaneous determination of apparatus dimensions and operating conditions for the optimal membrane-assisted reactive separation process. For the abovementioned case study the energy consumption can be reduced by up to 60 % lowering the production costs (objective function) in comparison to the benchmark process consisting of one continuous reactor and four distillation columns.

### Contact:

johannes.holtbruegge@bci.tu-dortmund.de  
philip.lutze@bci.tu-dortmund.de  
andrzej.gorak@bci.tu-dortmund.de

### Publications:

Holtbrügge J. et al., Process Analysis of Membrane-Assisted Reactive Distillation: Transesterification of Propylene Carbonate, 2<sup>nd</sup> European Energy Conference 2012, Maastricht, NL  
Holtbrügge J. et al., Modeling, Simulation and Exp. Investigation of a Reactive Hybrid Process for the Production of Dimethyl Carbonate, 11<sup>th</sup> Int.Symp.Process Systems Eng., 2012, Singapore

## Aqueous two-phase extraction of monoclonal antibodies

### Design of a multi-stage aqueous two-phase extraction

Jan Mündges, Sultan Mohammad, Tim Zeiner and Andrzej Górak

During the past years, the therapeutic application of monoclonal antibodies (mAbs) has increased. Through an intensified research on upstream-processing, the antibody concentration has significantly been enhanced in the fermentation broth. Hereby purification of mAbs became the most challenging step in the production process accounting for 50-80 % of the total costs. Aqueous two-phase systems (ATPS) are a promising technology for mAb purification featuring mild extraction conditions, large capacity and economical benefits. Aim of this research is the development of a simulation tool for modeling the extraction of mAbs using ATPS.

MABs are biologically active proteins produced by plasma cells in response to the presence of foreign substances. Several diseases like cancer, asthma or autoimmune diseases are already treated by antibodies and nearly all marketed antibodies are produced by mammalian cell cultures. The purification became the most challenging step in the manufacturing process since conventional unit operations like preparative chromatography are often limited by their capacity. An efficient alternative is given by the extraction of mAbs with aqueous two-phase systems.

ATPS are a promising option for the improvement of mAb purification. By mixing two different hydrophilic polymers or a hydrophilic polymer and a salt in water, two liquid phases can be formed which both exhibit an aqueous character. Purification of the target product is achieved because of a different distribution of product and impurities between both phases. Especially for sensitive products ATPS are a good alternative because of mild separation conditions at high capacity.

In this research project an ATPS comprised of polyethylene glycol, a phosphate salt and water is applied for the extraction of a mAb named AK1. Essential for the design of an aqueous two-phase extraction is a fundamental knowledge of substance properties, liquid-liquid equilibrium data as well as distribution of target component. The influence of relevant parameters like polymer molecular weight, phase composition, pH value and initial AK1 concentration, is investigated, to characterize the extraction.

Single-stage extraction experiments with purified AK1 showed, that the solubility of AK1 in the ATPS is the most limiting measure concerning the choice of extraction

parameters. The most significant impact on solubility is the pH value. A value of pH=6 was found out to offer the best solubility of AK1 in the ATPS (Figure 1).

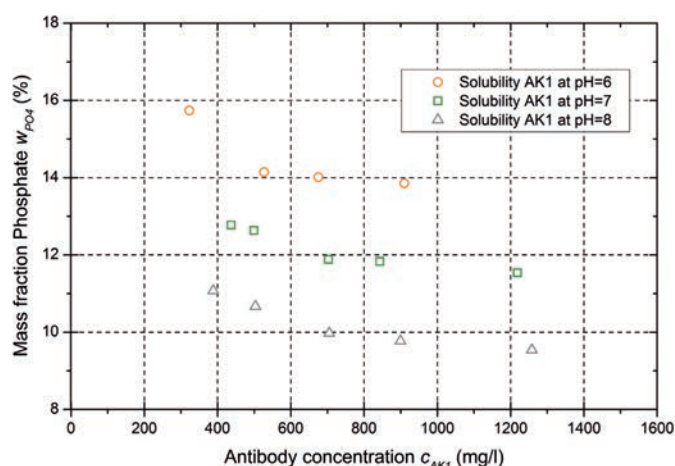


Figure 1: Solubility of AK1 in an aqueous phosphate solution in dependency of pH value.

After determining the rather small operating range for the extraction it was found out, that the impact of AK1 initial concentration on the system properties is negligibly small. Furthermore the choice of PEG molecular weight has no significant effect on the partition of AK1 in the investigated range.

In future investigations, the aqueous two-phase extraction will be performed with cell supernatant from Chinese hamster ovary cells. Especially the addition of sodium chloride is a promising parameter to influence the distribution of AK1 and hereby increase the selectivity of the extraction. Furthermore an equilibrium-stage model is going to be validated in multi-stage experiments executed in a mixer-settler unit present at our laboratory. The simulation of a multi-stage extraction is a powerful tool to simplify the design of extraction of antibodies in aqueous two-phase systems mainly reducing the experimental effort.

#### Contact:

jan.muendges@bci.tu-dortmund.de  
tim.zeiner@bci.tu-dortmund.de  
andrzej.gorak@bci.tu-dortmund.de

#### Publications:

Mündges J. et al., Experimental and theoretical investigation of antibody distribution in aqueous two-phase systems, AICHEM 2012, Frankfurt

Mündges J. et al., Untersuchung der einstufigen Extraktion eines Antikörpers in wässrigen Zwei-Phasen Systemen, ProcessNet-Jahrestagung und 30. DECHEMA-Jahrestagung der Biotechnologen 2012, Karlsruhe

## Ionic Liquids

### Extraction of 1,3-Propanediol Using Ionic Liquid-Based Aqueous Two-Phase Systems

Anja Müller and Andrzej Górak

The separation of 1,3-propanediol from fermentation broth is challenging because of its high polarity and high boiling point. Thus far, extraction has not been considered as potential separation method because of the extremely low solubility of 1,3-propanediol in organic solvents. However, ionic liquid based aqueous two-phase systems could be used to overcome this limitation. Hence, the aim of the present study was to investigate the ability of water miscible ionic liquids to build aqueous two-phase systems for the separation of 1,3-propanediol.

The ability of different ionic liquids to form aqueous two-phase systems using a mixture of  $K_2HPO_4$  and  $KH_2PO_4$  as the second phase forming component and the extraction performance for 1,3-propanediol were investigated at a temperature of 310.15 K (see figure 1).

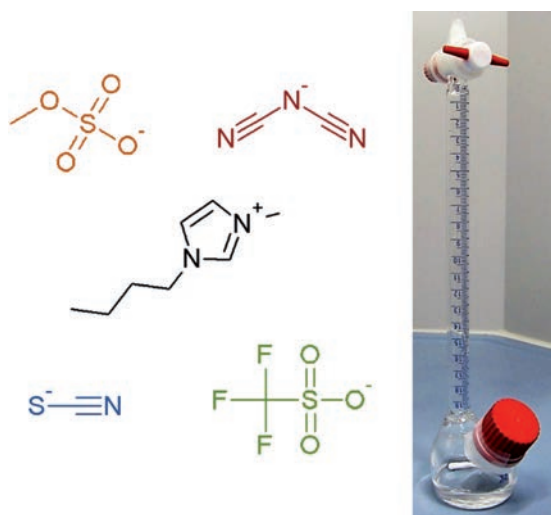


**Figure 1:** Examples for the used ionic liquids ( $[Im_{4,1}]^+$ ,  $[CF_3SO_3]^-$ ,  $[N(CN)_2]^-$ ,  $[SCN]^-$  and  $[CH_3SO_4]^-$ ) (left), extraction vessels (right).

All of the studied ionic liquids formed aqueous two-phase systems; however, with different sizes of the miscibility gaps. The location of the binodal curve turned out to be dependent on the polarity or hydrogen-bond accepting strength of the ionic liquid. Here, the influence of the anion and cation were comparable. Figure 2 shows exemplarily four selected binodal curves.

The distribution coefficients of 1,3-propanediol for the investigated systems were between 1.5 and 27.7. Consequently, the ionic liquid-rich phase contained more 1,3-propanediol than the phosphate-rich phase. The

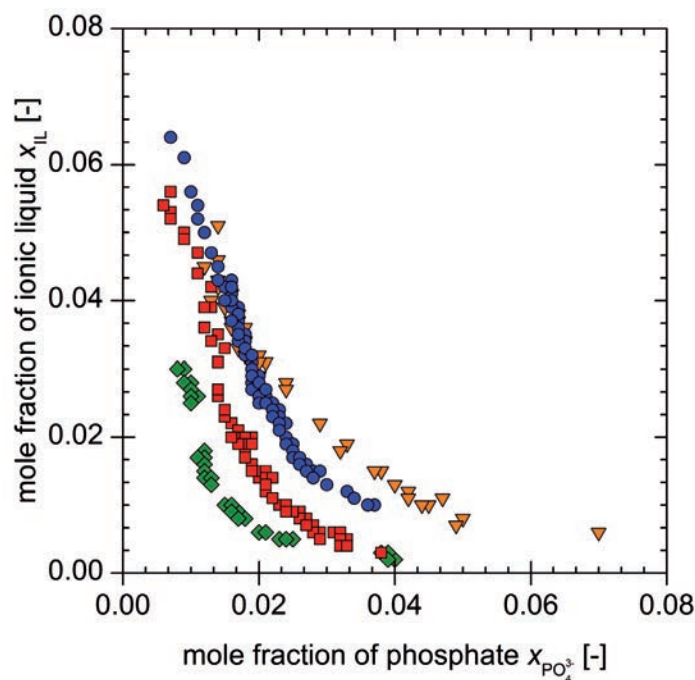
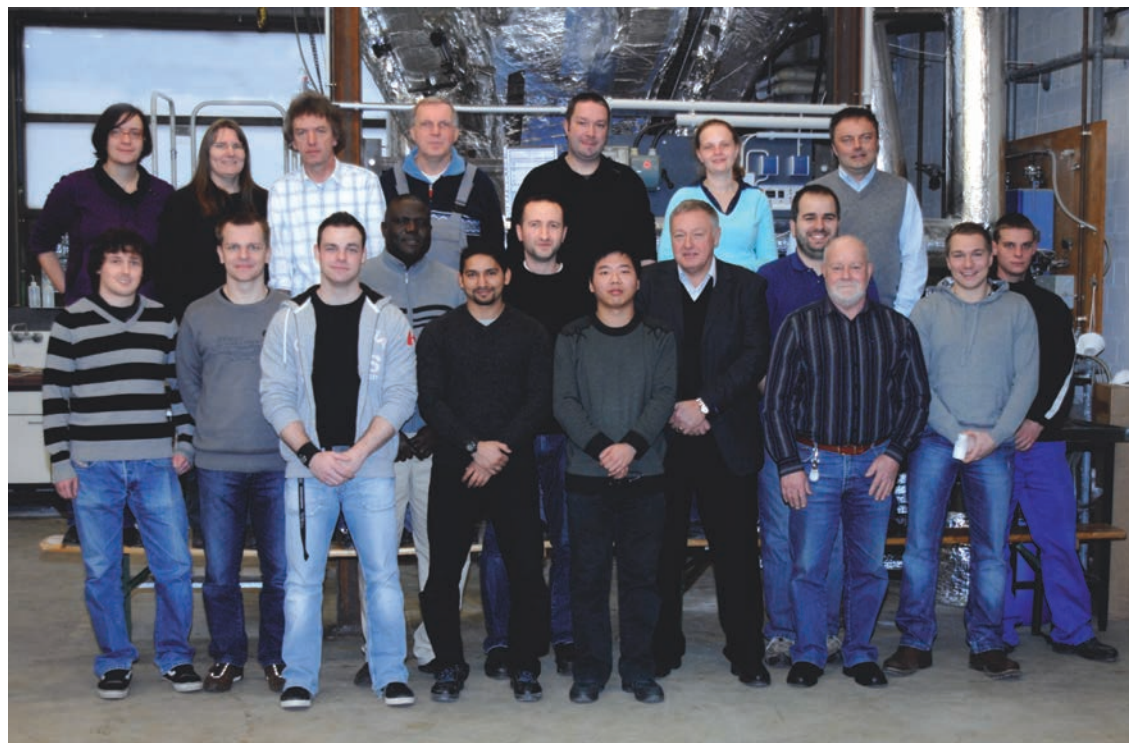


**Figure 2:** Binodal curves for different anions combined with  $[Im_{4,1}]^+$ :  $\blacklozenge$   $[CF_3SO_3]^-$ ,  $\blacksquare$   $[N(CN)_2]^-$ ,  $\bullet$   $[SCN]^-$  and  $\blacktriangledown$   $[CH_3SO_4]^-$ .

distribution coefficient of 1,3-propanediol also turned out to depend on the polarity or hydrogen-bond accepting strength as it increases with an increase in the polarity or hydrogen-bond accepting strength of the anion or cation (see figure 2). However, the influence of the anion is greater than that of the cation.

To select an appropriate ionic liquid, a compromise between the phase forming strength and extraction performance for 1,3-propanediol has to be made. The amounts of ionic liquid and phosphate to build the two phases have to be in an adequate magnitude by a satisfying distribution coefficient of 1,3-propanediol.



## Mechanical Process Engineering (MV)

## Characterization of dynamic mixers by the optical measurement of droplet size distributions of emulsions

Jörg Hillmann, Monika Sellerberg, Peter Walzel

When continuously dispersing low viscous liquids in high viscous liquids, often narrow droplet size distributions (DSD) are desired. One option to determine the DSD, reflecting the quality of an emulsion can be obtained by image evaluation. Microscopic images of emulsions show the contour of several droplets as rings usually overlapping in different field depth. Standard image analysis tools are not able to separate overlapping individuals and to contain the evaluation range to a given focal plane.

Dynamic mixers for their flexibility are suitable to form emulsions from two continuous feed streams, see figure 1. To get a dispersion of low viscous liquid in high viscous systems a close DSD is favored. The Sauter mean diameter depends on the liquid properties, operating parameters and the geometry of the inserts of the dynamic mixer.

$$d_{32} = f(D, n, \sigma, \eta, \dot{V})$$

Investigations are carried out with silicon oil and water using different pin and tooth mixer designs.



Figure 1: Design of a dynamic mixer.

To receive the DSD of such emulsions with an optical measurement technique an automated analysis of the images is necessary. The standard analysis tools for particle measurement from images require separated particles. Overlapping or agglomerated particles could not be separated in the analysis. Solid particles are usually completely dark, whereas droplets on microscopic images just appear as dark rings with a light center as can be seen in the images in figure 2. An automated analysis

of emulsion images was implemented in Matlab® by a modified Hough-transformation. An example for the identification of the droplets is given below. The program was validated with images of glass spheres with known diameter.

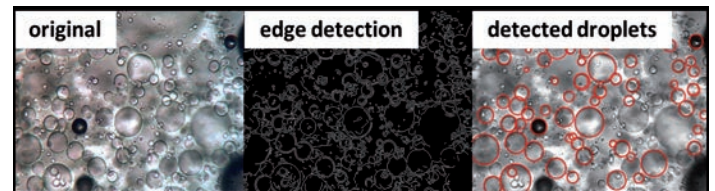


Figure 2: Example droplet identification with the automated analysis tool for emulsion images.

The comparison of the tooth- and pin-mixers by using the automatic evaluation tool for the droplets shows a significant effect on the DSD caused by the geometry of the mixer, mutually based on a different radial mixing behavior, see figure 3.

The mean drop sizes of the DSD generated by the tooth-mixer are twice as high as the mean droplet sizes produced by the pin-mixer for the same rotor speed, although torque measurements shows that the specific work of the tooth mixer is about 20% higher. However, no significant change of the distribution width is visible.

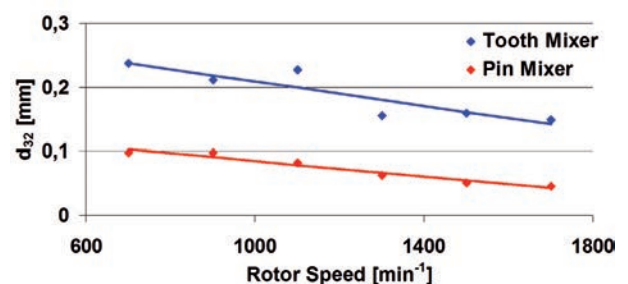


Figure 3: Effect of the variation of the rotor speed on the sauter mean diameter by using the tooth- and the pin-mixer

### Publications:

Hillmann, J., Sellerberg, M., Walzel, P., Characterization of dynamic mixers by the optical measurement of droplet size distributions of emulsions, 8th ECCE, September 25 - 29, 2011, Berlin/Germany, Oral Presentation.

### Contact:

joerg.hillmann@bci.tu-dortmund.de

monika.sellerberg@bci.tu-dortmund.de

## CFD-Simulation of the electrostatic precipitation process

### Modelling the corona-quenching effect in coaxial wire-tube-configuration

Sven Kaiser, Hans Fahlenkamp, Peter Walzel

The design of electrostatic precipitators (ESP) comes along with certain difficulties, especially if the intended operational conditions are characterized by the presence of a very high load of particles or droplets. In this case the high amount of particle bounded charge leads to a significant disturbance of the corona development causing a loss of precipitation efficiency. This effect is known as Corona-Quenching. The objective of this work is the development of a numerical model based on Computational Fluid Dynamics (CFD) and capable to cover this effect.

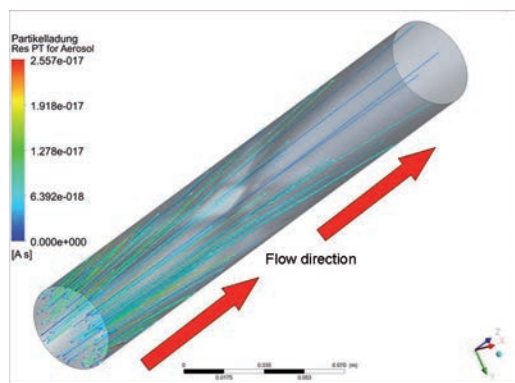


**Figure 1:** Particle trajectories in a wet ESP of coaxial wire-cylinder configuration. The color-scheme of the trajectories represents different loads of charge bounded to the particles.

The model makes use of an Euler-Lagrange-approach to simulate the fluid flow and the particle flow respectively (figure 1). Various simulations are performed with different parameters such as the applied voltage, the particle load or the geometric dimensions.

The impact of the former mentioned parameters on the current-voltage-characteristics and the precipitation efficiency is computed and compared to experimental results reported in the literature. In addition a pilot-plant was constructed in cooperation with the IUTA institute in Duisburg to realize measurements in a wide range of parameters relevant for industrial applications.

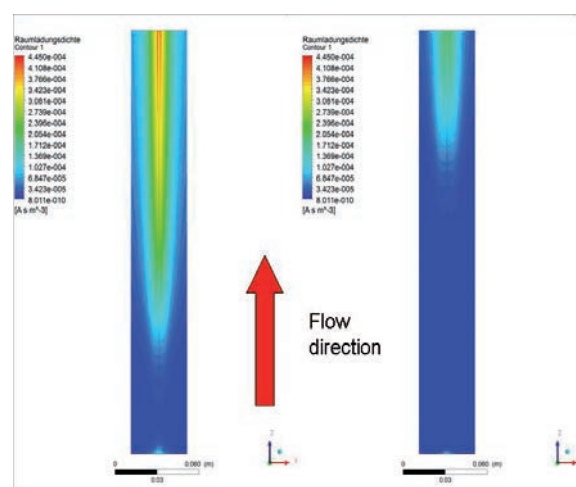


**Figure 2:** Distribution of the space charge density in a cross section of a laboratory scale precipitation unit under two different quenching conditions.

One of the main tasks is the development and implementation of a corona-sub-model to describe the overall amount of ions produced inside the corona, with the objective to determine the Dirichlet-boundary-condition necessary to calculate the distribution of ions under different quenching conditions (figure 2).

#### Publications:

Kaiser S., Fahlenkamp H., CFD modeling of the electrical phenomena and the particle precipitation process of wet ESP in coaxial wire-tube configuration, International journal of plasma environmental science and technology, october 2011  
Majid, M., Rojek, A., Wiggers, H., Walzel P., Visualisierung der Rücksprühvorgänge in Staubschichten in Elektrofiltern, Chemie Ingenieur Technik, 2010

#### Contact:

Sven.kaiser@bci.tu-dortmund.de  
Peter.walzel@bci.tu-dortmund.de

## Particle Classification in a high viscous environment

### *A Novel System for Particle Separation in a Laminar Tube Flow with Downstream Enlargement*

Paul Matulka and Peter Walzel

Particle classification is difficult when the density difference between particle and a highly viscous suspending fluid is almost negligible. Classical sieving methods are practically prohibited due to the strong interaction between particles the fluid and the meshes. Sedimentation is not applicable when the particles and the fluid have almost same densities and the settling velocities are low. Such problems however arise in biological and chemical systems, i.e. gel particle separation from polymers, size separation of particles in pharmaceutical emulsions etc. In such cases, the separation can be achieved in laminar tube flows by single or multiple tube arrangements.

In a laminar tube flow particles find their equilibrium radius depending on the particle to tube size ratio. While small particles migrate from the center of the flow towards the wall and find their equilibrium radial position, large particles are transported towards a more central streamline in the tube (see Figure 1).

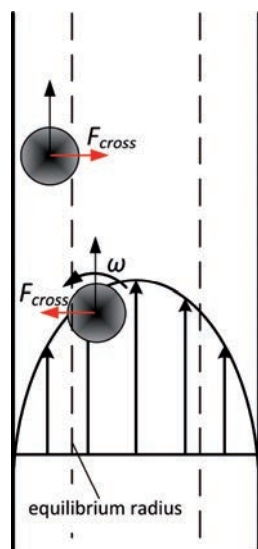


**Figure 1:** Particles find the radial position on their equilibrium radius in a laminar tube flow.

However a particle free zone near the wall remains.

In such a way, the particles separate and form ring zones within the suspension of the dispersed particles. The radii of these ring zones depend on the particle diameter. Particle migration is observed when the ratio of particle

to tube diameter is  $0.08 < d/D < 0.4$  at low but nonzero Reynolds numbers  $10 < Re < 30$ . In a downstream enlargement the particles follow divergent streamlines and are classified in downstream annular collection arrangements and also a clear flow can be removed. Figure 2 shows the separation system.

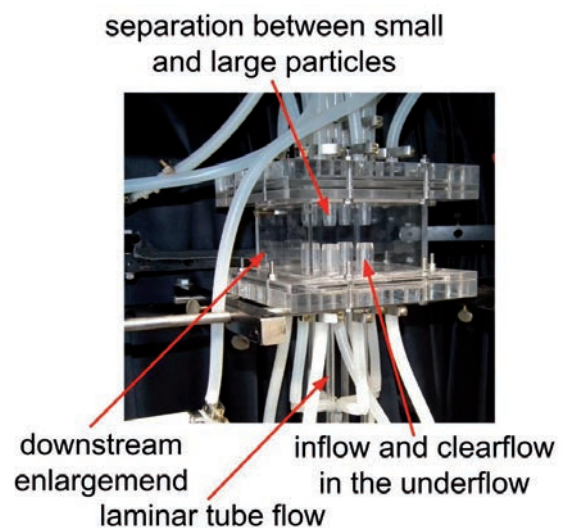


**Figure 2:** Downstream Enlargement with four annular collecting flow tubes. Separation between small and large particles in the downstream enlargement takes place and a clear flow is removed in the underflow.

The optimum process parameters for the separation system were found. Particles should have a minimal size ratio of particles of  $d_i/d_{i+1} \geq 0.03$  and the particles should not be smaller than  $d/D = 0.12$ . An optimal tube Reynolds number range could be confirmed. With increasing tube Reynolds number at  $Re > 16$ , the classification effect is still visible but fading.

Publications:  
Matulka, P., Du, X., Walzel, P.: Particle Motion and Separation in a Laminar Tube Flow with Downstream Enlargement, Chemical Engineering Science, 66 (2011), 5930-5937

## Wet Scrubber Simulation

*A novel method to map wet scrubbers into computer fluid dynamics*

Damian Pieloth, Gerhard Schaldach, Tim Neumann, Peter Walzel

The removal of dust particles and droplets from exhaust gases still challenges the design and optimization of wet scrubbers. The separation efficiencies of those apparatus have to fulfill current and future environmental requirements. Water and energy consumption have to be reduced. Laboratory experiments with pilot plant wet scrubbers cover only a very limited space of operating conditions. CFD simulations can supplement experiments in wet scrubber design. We developed a novel method to map wet scrubbers into commercial and common CFD software. An Euler-Lagrangian approach is used. The dust particles are homogeneously imbedded into the Euler-Phase. The scrubbing process is based on the collection efficiency of a single droplet. This simulation method is very fast, even when applied for simulation of a whole wet scrubber arrangement. It is applicable to various wet scrubber types and shows a good agreement with experiments [1].

In a given gas flow regime the collision efficiency of a dust particle with a droplet cannot be calculated analytically as a whole but has to be measured by experiment or calculated numerically, e.g. by CFD simulations as in figure 1.

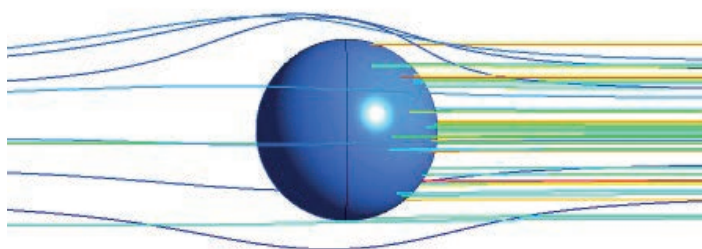


**Figure 1:** ANSYS CFX simulation of collision between dust particles and a droplet. Smaller particles with less inertia (blue) follow the streamlines around the droplet while bigger particles (red) collide with the droplet.

Knowing the collision efficiency  $\eta$  of dust particles with every single droplet along its trajectory within the scrubber as a function of the droplet Reynolds-Number  $Re_d$  and Stokes parameter  $\psi$ , we can calculate the separation effect caused by a polydisperse spray of the washing liquid within the wet scrubber more precisely. For a given droplet Reynolds-Number  $Re_d$   $\eta$  can be parameterized as

$$\eta = (\psi / (\psi + a))^b$$

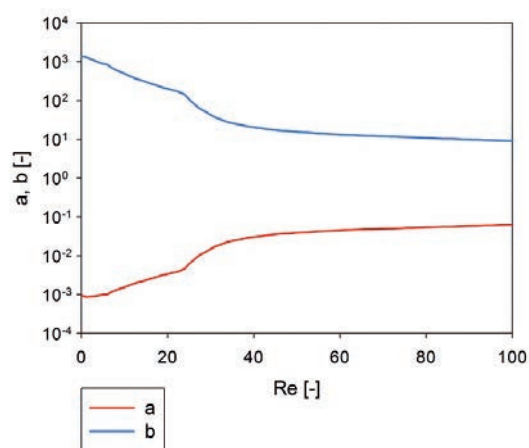


**Figure 2:** ANSYS CFX calculated a and b for wide range of droplet Reynolds-Number  $Re_d$ .

The CFD simulation follows the trajectories of individual droplets. Exceeding from known DSD's one can simulate different wet scrubber types under different operational conditions, see figure 3.

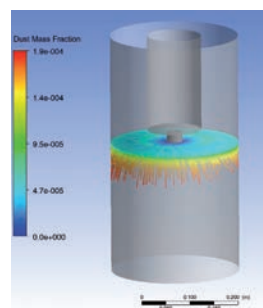


**Figure 3:** ANSYS CFX simulation of rotary wet-scrubber. Droplets leaving the rotary wheel spaying system collect dust particles during their pathway within the scrubber. Hence the dust load of the droplet increases (pictured with tracks of the droplets starting with blue i.e. low dust load, and become red at higher particle load).

This kind of CFD simulation method can be also applied to optimize nozzles for powder entrainment into sprays as in forming PU (polyurethane) foams [2].

**Contact:**

damian.pieloth@bci.tu-dortmund.de  
gerhard.schaldach@bci.tu-dortmund.de  
peter.walzel@bci.tu-dortmund.de

### Publications:

- [1] Pieloth, D., Kohnen, B., Schaldach, G., Walzel, P., CFD-Simulation von Nasswäschern, Chem. Ing. Tech., 2012, 84(1-2), pp. 127–137.  
[2] Schaldach, G., Pieloth, D., Kohnen, B., Großmann, M., Walzel, P., CFD-Simulation der Feststoffeinbindung in einen Sprühstrahl, Chem. Ing. Tech., 2011, 83(6), pp. 893–899.





## Technical Biochemistry (TB)

## Towards a platform organism for terpenoid production

*In silico* comparison of metabolic networks of *E. coli* and *S. cerevisiae* as potential hosts

Evamaria Gruchattka, Oliver Kayser and Verena Schütz

Terpenoids are one of the largest classes of natural products and possess important medicinal and industrial applications. The heterologous production of plant terpenoids in microorganisms is a concept to overcome supply problems and high purification costs as several compounds are rare and produced only in low amounts in plants. Our focus is on the development of a platform organism for the efficient supply of isopentenylpyrophosphate (IPP), the biosynthetic precursor of all terpenoids. *E. coli* and the yeast *S. cerevisiae* are potential hosts that use two different pathways to produce IPP. (Fig 1.)

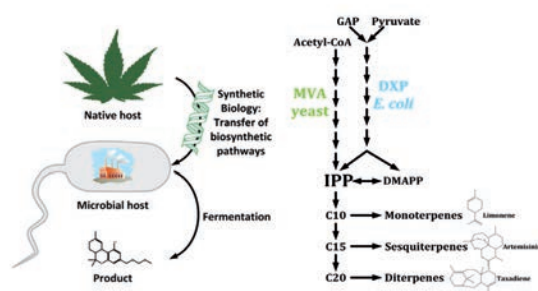


**Figure 1:** Synthetic biology for the production of plant terpenoids. Yeast and *E. coli* use different pathways to supply the common terpenoid precursor IPP.

*E. coli* and *S. cerevisiae* are compared by means of elementary flux mode analysis (EMA) regarding their metabolic potential to supply IPP. EMA allows the calculation of a solution space containing all steady state flux distributions of a metabolic network considering stoichiometry, topology and thermodynamics (Fig. 2).

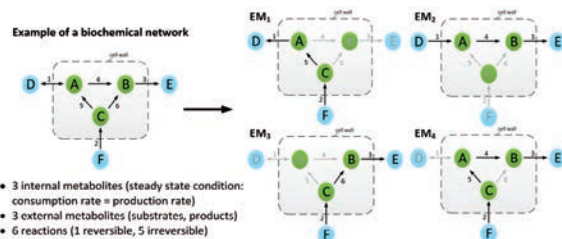


**Figure 2:** Concept of elementary flux mode analysis

Models of the central carbon metabolism of both organisms were constructed considering current knowledge from genome scale models and literature. The theoretical maximum IPP yield was calculated. Exchange and combination of the DXP and MVA pathway were analyzed. (Fig. 3)

**Contact:**  
 verena.schuetz@bci.tu-dortmund.de  
 evamaria.gruchattka@bci.tu-dortmund.de  
 oliver.kayser@bci.tu-dortmund.de

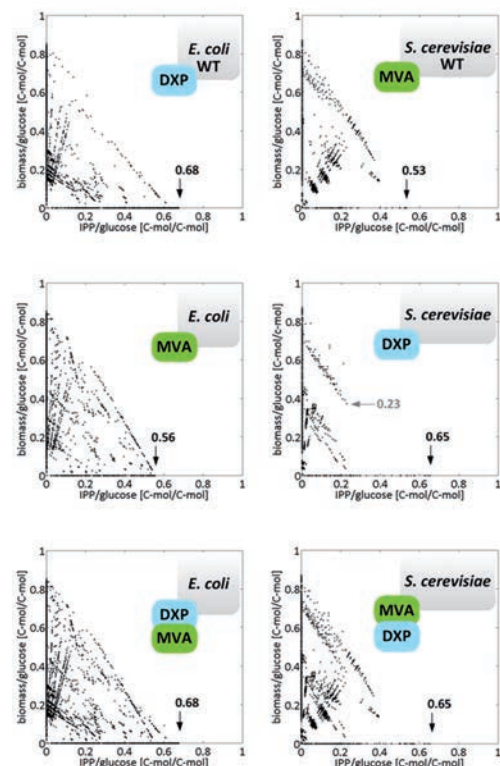


**Figure 3:** IPP and biomass yields for the obtained elementary modes with glucose as carbon source. *E. coli* wild type shows a higher potential to supply IPP than *S. cerevisiae* wild type, with and without biomass formation. The exchange of DXP and MVA pathway lowers the maximum theoretical carbon yield for *E. coli*. The exchange enhances the YIPmax for *S. cerevisiae*, however, the maximum theoretical IPP yield with biomass formation is lowered. The exchange of the terpenoid pathways is stoichiometrically not efficient.

The data obtained from EMA will now be used for the rational identification of targets for metabolic engineering. A proof of concept will be performed using patchouli synthase producing the plant sesquiterpene patchouli.

**Publications:**  
 Towards a platform organism for terpenoid production – *in silico* comparison of metabolic networks of *E. coli* and *S. cerevisiae* as potential hosts, Conference: Applied Synthetic Biology in Europe, Barcelona, Spain, 06. - 08. February 2012, book of abstracts: page 48  
*E. coli* versus *S. cerevisiae* – On the Competition for Terpenoid Production, Conference: New Biotrends to smarter drugs, Dortmund, Germany, 08. - 09. December 2011, book of abstracts: page 25

## Human tetrahydrocannabinol metabolites

*An inexpensive way to produce novel drug candidates*

Torsten T. Arndt, Armin Quentmeier and Oliver Kayser

*The human metabolites of tetrahydrocannabinol are responsible for a part of the effects of cannabis use and thus are interesting medicinal candidates. We showed that production of 11-hydroxy tetrahydrocannabinol with recombinant whole cells expressing human cytochrome P450 is possible.*

The phytocannabinoids produced by *Cannabis sativa*, with the most prominent example of tetrahydrocannabinol (THC), exert a number of medically interesting effects on humans and can be used to treat nausea and vomiting during cancer therapy, eating disorders, spasms, pain, and tremor.

THC in the human body is readily converted to its metabolites 11-hydroxyTHC and 11-nor-9-carboxy-THC by cytochromes P450. These metabolites play an important role in the effects of THC use. Being able to produce them in large scale might provide new approaches to old medicinal effects and offer a way to use the beneficial impact of THC without the psychoactive effects.

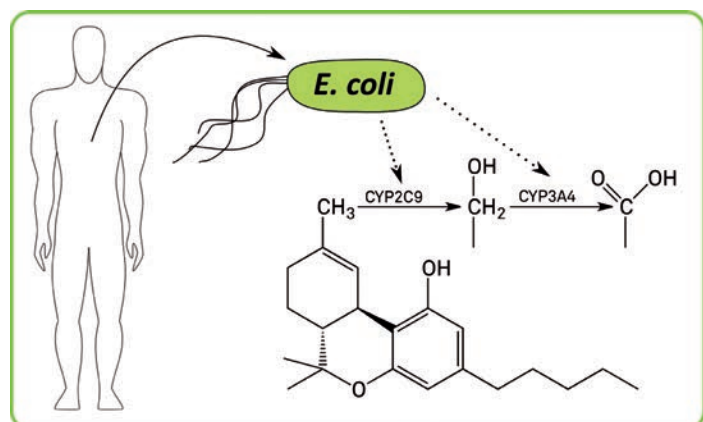


**Figure 1:** Human genes are introduced into *E. coli*, which is then used as biocatalyst to produce human metabolites of tetrahydrocannabinol.

*Escherichia coli* DH5 $\alpha$  was used to express a modified human Cytochrome P450 2C9. Expression was optimized by fine-tuning the oxygen concentration in the medium, which shows a significant influence on the amount of correctly folded enzyme. The highest enzyme concentration of 1100 nM was achieved under microaerophilic conditions.

Cytochromes P450 require a supply of the redox cofactor NADPH to function. Although *in vitro* conversion of THC with recombinantly expressed P450 is possible using a NADPH regenerating enzyme system, this alternative is very costly. Using just glucose as energy source, non-growing cells without a nitrogen source were able to convert THC efficiently and produce 11-hydroxy tetrahydrocannabinol up to a concentration of about 55 mg/L with a turnover rate of  $1.7 \times 10^{-2} \text{ s}^{-1}$  within 24 h.

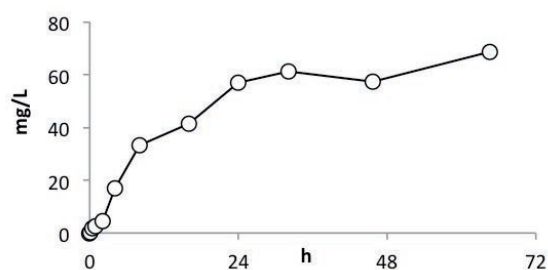


**Figure 2:** Time course of 11-hydroxy tetrahydrocannabinol concentration. Incubation of *E. coli* DH5 $\alpha$  pCW2C9 expressing 1030  $\mu\text{M}$  Cytochrome P450 2C9 in potassium phosphate buffer with 10 g/L Glucose and 314 mg/L tetrahydrocannabinol.

We could show that conversion of tetrahydrocannabinol using whole cells expressing recombinant human cytochromes is a promising approach to synthesize metabolites. This might open the opportunity to use these metabolites as novel drugs and allow a cannabinoid-treatment with less side effects.

### Publications:

Andt, T. T., Quentmeier, A., Kayser, O. (2012) Towards the economic production of a human tetrahydrocannabinol metabolite. Poster Presentation – Third Annual CLIB Retreat, Bergisch-Gladbach 2012, S. 18.

### Contact:

torsten.arndt@bci.tu-dortmund.de  
armin.quentmeier@bci.tu-dortmund.de  
oliver.kayser@bci.tu-dortmund.de





## Technical Chemistry A (TCA)

## Homogeneously catalysed Hydroformylation of 1-Dodecene

### Catalyst Performance and Recycling

Yvonne Brunsch, Arno Behr

This work is part of the Sonderforschungsbereich Transregio 63 (SFB/TR 63) „Integrated chemical processes in liquid multiphase systems“ (InPROMPT), which is a joint project of chemistry and process engineering. The research activity focuses on the development of an innovative process for the production of aldehydes via homogeneous, transition-metal catalysed hydroformylation of higher olefins [1].

The challenging task of the homogeneously catalysed hydroformylation of higher olefins is the efficient combination of the reaction and a subsequent separation step for catalyst recovery and recycling. In our investigations thermomorphic solvent systems (TMS) are used [2, 3]. The rhodium catalysed hydroformylation of 1-dodecene serves as model reaction (Fig. 1).

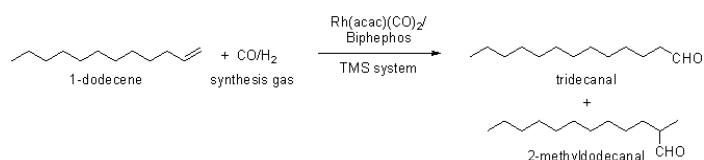


Figure 1: Reaction equation of the rhodium catalyzed hydroformylation of 1 dodecene

The principle of TMS systems implies, that the reaction runs homogeneously in one phase, whereas two phases exist during separation step for catalyst recycling.

The reaction performance is investigated by varying the substrate/metal ratio during hydroformylation reaction (Fig. 2).

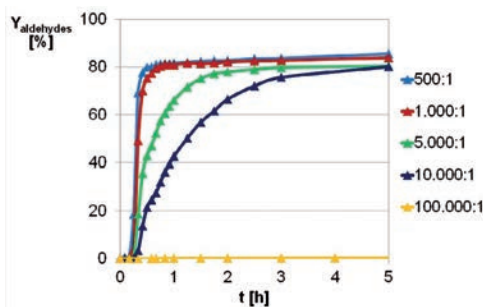


Figure 2: Variation of the substrate/metal ratio.

[1] [www.inprompt.tu-berlin.de](http://www.inprompt.tu-berlin.de)

[2] A. Behr, G. Henze, R. Schomäcker, Adv. Synth. Catal. 2006, 348, 1485-1495

[3] A. Behr, G. Henze, L. Johnen, C. Awungacha, J. Mol. Catal. A: Chemical, 2008, 285, 20-28.

The reaction is faster, when high catalyst concentrations are employed.

The concept of TMS systems was successfully applied to the hydroformylation of 1 dodecene. Figure 3 shows a catalyst recycling in 8 recycling runs. It is demonstrated, that no loss in catalyst activity is observed.

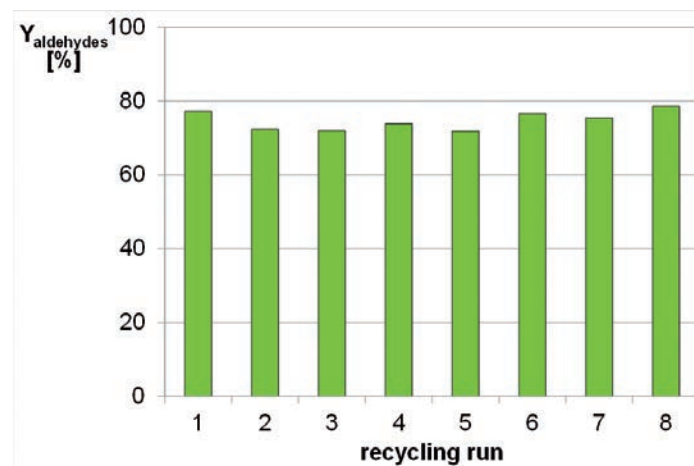


Figure 3: Catalyst recycling in 8 recycling runs [4].

It is demonstrated, that in TMS systems catalyst separation and recycling is possible for the hydroformylation of higher olefins. The investigation of the chemical fundamentals was integrated into the interdisciplinary design and construction of a miniplant. Ongoing studies imply for example the optimisation of process parameter and the application to further TMS systems, substrates or reaction systems.

#### Publications:

[4] E. Schäfer, Y. Brunsch, G. Sadowski, A. Behr, Industrial and Engineering Chemistry Research, 2012, accepted  
Y. Brunsch, A. Lux, A. Behr, Tetrahedron Letters, 2012, 53, 2680-2683

#### Contact:

yvonne.brunsch@bci.tu-dortmund.de  
arno.behr@bci.tu-dortmund.de

## Cross metathesis of methyl undec-10-enoate with dimethyl maleate

*A new protocol with nearly quantitative yields*

Arno Behr, Stephanie Krema

Fats and oils represent the largest share with 40% of renewable raw materials in the chemical industry. Especially, the olefin cross metathesis with oleochemicals offers a versatile synthesis approach to prepare value added starting materials from renewable raw materials. The cross metathesis of fatty acid derivatives yield  $\alpha,\omega$ -difunctional monomers, which can be processed into polymers.

The cross metathesis of methyl undec-10-enoate **1** with dimethyl maleate **2** results in the products dimethyl dodec-2-enedioate **3** and methyl acrylate **4** (Fig.1).

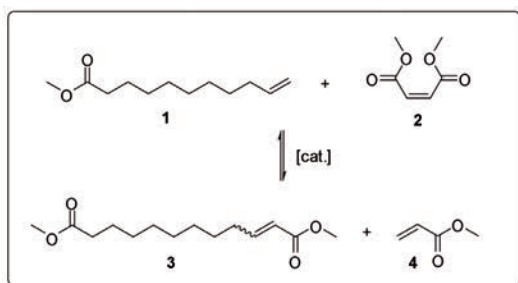


**Figure 1:** Cross metathesis of methyl undec-10-enoate **1** with dimethyl maleate **2**.

In this case the considered cross metathesis was optimized with respect to the difunctional product **3**, which could be used as a starting material in the synthesis of polymers.

We examined several reaction parameters toward the desired product, which included a systematically variation of catalyst screening, catalyst concentration, reaction time, reaction temperature, reaction solvent and the ratio of the substrates **1** and **2**.

A reaction temperature of 80°C yield in nearly quantitative yields of the product **3**. Other side-products, such as the self metathesis products of **1** could not be observed at this temperature. To assess more accurately the course of the reaction, various time experiments were recorded. The reaction could be completed within one hour.

The amount of the solvent plays a significant role in this cross metathesis. The desired product is created only with a substrate concentration higher/equal to 60% in nearly quantitatively yields.

At the end of our investigations in the reaction optimization the catalyst concentration was investigated to reduce the amount of catalyst (Fig.2).

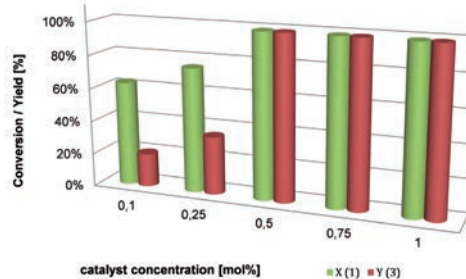


**Figure 2:** Variation of the catalyst concentration in the investigated cross metathesis.

In the cross-metathesis of methyl undec-10-enoate **1** with dimethyl maleate **2** the desired  $\alpha,\omega$ -difunctional product **3** can be generated under mild reaction conditions. With a reaction temperature of 80°C in one hour with a catalyst loading of 0.75 mol% of a standard homogeneous ruthenium metathesis catalyst nearly quantitative yields are achievable.

**Financial supported by BMELV in cooperation with Emery Oleochemicals**

### Publications:

A. Behr, S. Krema, "Metathesis applied to unsaturated lipid compounds", *Lipid Technol.*, 2011, 23, 156

A. Behr, S. Krema, "Cross metathesis of methyl undec-10-enoate with dimethylmaleate: A new protocol with nearly quantitative yields", in preparation

### Contact:

arno.behr@bci.tu-dortmund.de

stephanie.krema@bci.tu-dortmund.de

## Homogeneously catalysed alkoxy-carbonylation of myrcene

*From renewable resources to odourous compounds*

Arno Behr, Leif Johnen, Andreas Wintzer

Chemical products based on renewable resources represent sustainable alternatives to common petrochemical products in chemical industry. The structural framework of terpenes is similar to that of petrochemical feedstocks and that is why they are promising sustainable alternatives. In many industrial processes the monoterpene myrcene is transformed to fine chemicals. Here we are presenting a carbonylation method that leads directly from olefins to alkyl esters. The alkoxy-carbonylation of myrcene is competing with myrcene isomerisation and that is why maximising ester selectivity was investigated.

Alkoxy-carbonylation is an atom economic carbonylation method with that mainly terminal alkenes can be transformed to different alkyl esters, depending on the used alcohol. Besides the alcohol which acts as a nucleophile, carbon monoxide is used which will be inserted into the carbon framework. These two easily available substrates together with the atom economy are making the alkoxy-carbonylation a useful way for producing esters out of alkenes.

The attractiveness of myrcene, the conjugated diene unit is, however, also a factor for negative effects such as isomerisation. Under specific reaction conditions the double bonds can change their position very fast. The required reaction temperature for the alkoxy-carbonylation is 140 °C and together with the yield rising co-catalyst acetic acid, isomerisation is the competing reaction to alkoxy-carbonylation (Figure 1).

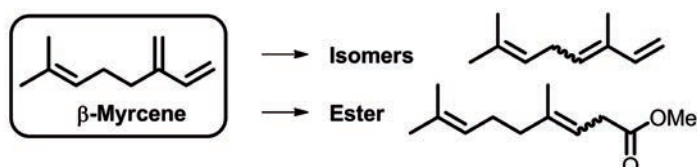


**Figure 1:** An important side reaction in the alkoxy-carbonylation of myrcene is the isomerisation of the starting material.

The methyl esters have a fruity odour, and the product variety is very high, because with methanol, isopropyl alcohol and tert-butyl alcohol, primary, secondary and even tertiary alcohols can be used as substrate.

With respect to the tendency of myrcene isomerisation we found that by choice of reaction conditions the isomerisation can be suppressed effectively. Given by the ratio of ester yield to isomer yield the selectivity was 0.7 at the beginning of our research. One important factor is the amount of acetic acid, 3 equivalents referred to a catalyst load of 0.5 mol% is a good compromise between high activity and relatively low isomerisation. Other important parameters represent the myrcene/methanol ratio and the carbon monoxide pressure. With a combination of all optimized parameters the ester/isomer ratio can be raised to 7.2 (Figure 2). That means it could be raised by a factor of 10.



**Figure 2:** With certain reaction parameters such as CO pressure, the ester selectivity can be maximised to a high ester/isomer ratio.

Our results underline that especially in flavor and fragrance chemistry monoterpenes are representing high potential starting materials. Along with atom economic syntheses, the use of easily available bulk chemicals and reuse of the homogeneous catalyst they provide sustainable chemistry which is one of the most important research areas in our time.

**Contact:**  
arno.behr@bci.tu-dortmund.de  
leif.johnen@bci.tu-dortmund.de  
andreas.wintzer@bci.tu-dortmund.de

**Publications:**  
Behr, A., Johnen, L., Wintzer, A., Willstumpf, A., Dinges, M., First alkoxy-carbonylation of the renewable myrcene: high selectivity through suppression of isomerisation, in preparation, (2012).

## Catalytic hydrogenation of carbon dioxide to formic acid

### Design and construction of a miniplant

Arno Behr, Kristina Nowakowski, Jennifer Haßelberg

Currently, formic acid is commercially produced by the carbonylation of methanol with the toxic carbon monoxide and the following hydration of methyl formate with water. A one-step alternative is the homogenous catalyzed hydrogenation of carbon dioxide. The use of carbon dioxide as a raw material for chemical syntheses is of particular interest: Carbon dioxide constitutes a non toxic and great available C1-building block for chemical syntheses.

For the conversion of the comparatively unreactive carbon dioxide to formic acid suitable homogenous catalysts and reaction conditions have to be found. Because of thermodynamically reasons a base such as dimethylamine, triethylamine or ammonia is necessary for the desired reaction (Fig.1).

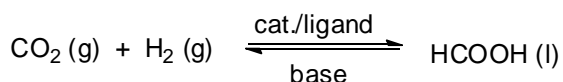


Figure 1: General chemical equation for the hydrogenation of carbon dioxide.

Therefore various homogeneous noble metals like rhodium, ruthenium and iridium with different oxidation levels have been investigated. **Laboratory studies** showed that the homogenous catalyst  $\text{Ru}(\text{acac})_3$  solved in water achieved the highest TON of 52.000 (total pressure 30bar ( $p(\text{CO}_2) = p(\text{H}_2)$ ), 25°C, t = 6h, triethylamine). An increasing concentration of the base enhanced the yield of formic acid. In addition the reaction conditions were optimized for a transfer of the reaction into a miniplant.

A continuous and adjustable **miniplant** for the production of formic acid by the hydrogenation of carbon dioxide has been designed and built. The three operation-units are: reaction, liquid-liquid separation and liquid-gas separation (Fig.2).



Figure 2: Photography of the miniplant for the continuous production of formic acid.

The reaction proceeds in a stirred tank reactor with an effective gassing stirrer. Both gases, carbon dioxide and hydrogen, are added with the assistance of a gas sparger. After the reaction two phases exist: one phase contains the homogeneous catalyst and the other the product formic acid. Based on the density difference, the two phases can be easily separated (liquid-liquid-separator) and the catalyst-phase can be recycled to the reactor.

This research work is part of the project "CO2RRECT" in which 18 parties work together for an efficient use of carbon dioxide as a carbon building block. The project is sponsored by the Federal Ministry of Education and Research.

Contact:  
arno.behr@bci.tu-dortmund.de  
kristina.nowakowski@bci.tu-dortmund.de  
jennifer.hasselberg@bci.tu-dortmund.de

## Efficient Hydroformylation of 1,3-Pentadiene

Arno Behr, Peter Neubert, Sarah Reinhold

Fossil feedstocks are the main source for organic basic compounds in chemical industries. However, as they are finite resources, a more flexible use is a major target. In this context, the efficient hydroformylation of 1,3-pentadiene, a well-known compound of the C<sub>5</sub>-cut of the naphtha-steamcracker, with synthesis gas has been investigated.

Hydroformylation is the most important homogeneously catalyzed reaction in industry giving aldehydes. It has been investigated by Otto Roelen in 1938 and it involves the addition of a carbon monoxide and a hydrogen group to an unsaturated molecule, such as olefins, alkynes or dienes.

When 1,3-pentadiene (1) is subjected to hydroformylation conditions, there are several possible products, arising from either 1,2- or 1,4-addition of CO and H<sub>2</sub>; however, there are two main products 2 and 3 (figure 1).

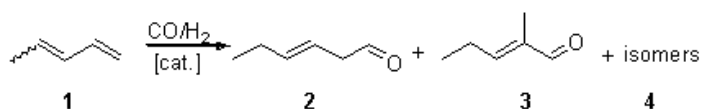


Figure 1: Main products in 1,3-pentadiene hydroformylation.

The products are known to exhibit odoriferous properties, which offer a broad application in industrial fragrance synthesis.

In a primary catalyst screening, the rhodium precursor Rh(CO)<sub>2</sub>acac turned out to be the most efficient. If it is used XANTphos as a ligand, the reaction provides yields up to 80% under 30 bar of synthesis gas.

Nevertheless, the reaction clearly affords a high metal to ligand ratio. When using Rh(CO)<sub>2</sub>acac with XANTphos as a ligand, the reactions requires high ratios of at least 1:20. After optimization of the reaction parameters, the kinetic behavior of the reaction gave further insights into the reaction course (figure 2).

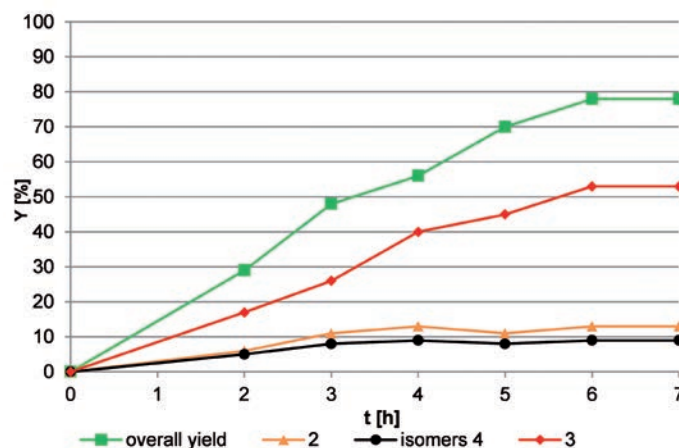


Figure 2: Kinetic behavior of the hydroformylation of 1,3-pentadiene.

It turned out, that the formation of all isomers proceeds totally independently with compound 3 as the clearly main product. On the other hand, the reaction is finished after 7 hours, giving yields up to 80%.

In conclusion we have developed an optimized piperylene hydroformylation which gives higher yields under clearly milder conditions, in comparison to contributions before, which suffers from low yields (60%) and extremely high pressures (up to 200 bar).<sup>[1]</sup>

[1] B. Fell, W. Rupilius, *Angewandte Chemie* **1969**, 81, 916.



## Technical Chemistry B (TCB)

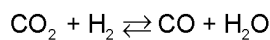
## Resource efficiency by using CO<sub>2</sub> as a raw material

### Application of adsorptive reactors for the reverse water-gas shift reaction

Sebastian Jung, Prof. David W. Agar

Unjustly, carbon dioxide is often considered purely as a waste product. It can, however, be activated to serve as a C<sub>1</sub> building block for chemical syntheses.

To increase the reactivity of the thermodynamically very inert CO<sub>2</sub>, it may be simply reduced to carbon monoxide with hydrogen from regenerative or other sources using the reverse water-gas shift reaction (rWGS):



An adsorptive reactor concept offers two considerable benefits for this reaction:

1. The reaction equilibrium is shifted to the product side by the *in situ* adsorption of water according to Le Chatelier's principle (see Figure 1). The reaction can thus be operated at 200-250°C rather than the 800°C necessary with conventional reactor technology.

2. The energy for the endothermic reaction is supplied at the pellet level by the enthalpy liberated in the exothermic adsorption step (see Figure 2).

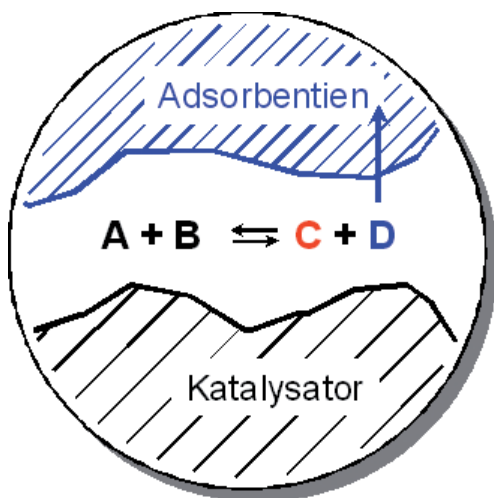


Figure 1: Schematic diagram of the *in situ* adsorption of by-products

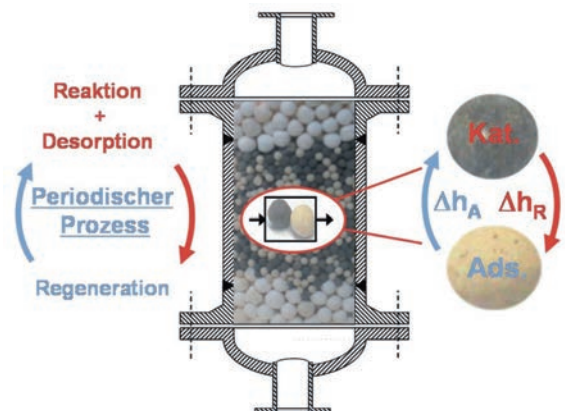


Figure 2: Adsorptive reactor for heterogeneously catalysed reactions

The synthesis gas thus generated has a wide variety of potential applications, for instance the Fischer-Tropsch synthesis of hydrocarbons, and, via the intermediate methanol using the methanol-to-olefins process, can be converted to conventional chemical feedstocks. These downstream processes provide the heat necessary to meet the demands arising in the adsorptive rWGS regeneration phase.

The results of a carbon-footprint-analysis indicates the potential to decrease the carbon footprint of olefins, such as ethylene and propylene, by about 2 kgCO<sub>2</sub>/kg olefin assuming that regeneratively manufactured hydrogen is used.

Both model simulations and experimental studies have been conducted to assess the performance of an adsorptive rWGS reactor. The 'proof of principle' has been demonstrated, although the space-time-yields of c. 0.0033 kgCO/(kg<sub>cat</sub>•h) are still too low.

The high costs of the hydrogen needed mean that this process is presently not economically competitive – a feature shared by most CO<sub>2</sub> chemistry. Nevertheless, in the future it could serve as a useful and flexible sink for excess hydrogen generated when power supply exceeds demand.

#### Publications:

S. Jung, S. Reining, S. Schindler, D. W. Agar, Ressourceneffizienz durch stoffliche Nutzung von CO<sub>2</sub>: Anwendung von adsorptiven Reaktoren für die reverse Water-Gas-Shift Reaktion, Processnet Jahrestreffen Reaktionstechnik Würzburg 14.-16.05.2012

#### Contact:

sebastian.jung@bci.tu-dortmund.de,  
agar@bci.tu-dortmund.de

## Selectivity enhancement by using permselective microcapsule

*A facile method to regulate the permselectivity of encapsulated catalyst*

Pavadee Pachariyanon and David W. Agar

Microencapsulation which is a technique that encloses an active substance within a coating material was used to modify the selectivity of an enclosed catalyst by manipulating the permselectivity of microcapsule membrane. Employing additional or multiple permselectivities could render the encapsulation of catalysts in microcapsules an even more powerful tool for improving the selectivity of the immobilised catalyst with the help of discriminating permeable membrane as a simpler alternative to the chemical modification of catalyst.

A permselective co-polymerised of polyacrylamide-alginate (pAAm-Alg) microcapsule was prepared by a double concentric nozzle. It was found that the optimum size of the pAAm-Alg microcapsule and the membrane thickness were found to be 3.2 mm and 234  $\mu\text{m}$  respectively (Figure 1)



Figure 1: Morphology of pAAm-Alg microcapsule.

The pAAm-Alg microcapsule membrane permitted the diffusion of glucose, maltose and dextran T1 but largely retained insulin,  $\alpha$ -lactalbumin and trypsin. The MWCO or size selectivity of the pAAm-Alg microcapsule membrane was thus narrowed to the range of 1.1-5 kDa, compared to the value of roughly 65 kDa for a purely calcium alginate membrane (Figure 2).

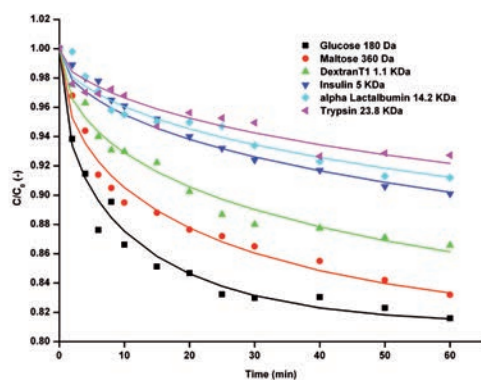


Figure 2: MWCO of pAAm-Alg microcapsule.

Considering other permselective properties of pAAm-Alg microcapsule, multicompetitive substrates selectivity of transesterification of fatty acid at different chain lengths with alcohols were selected as a test system. The results exhibited that while free enzyme show high selectivity toward long chain fatty acid, encapsulated enzyme in pAAm-Alg microcapsule exhibit high selectivity toward short chain fatty acid which is attributed to the hydrophilic property of pAAm-Alg microcapsule membrane. Moreover, by modify pAAm-Alg membrane with hydrophobic monomer isopropyl acrylamide (IPPAAM), the modified microcapsule pAAm-IPPAAM-Alg microcapsule shift its permselectivity toward long chain fatty acid while retain the property of encapsulated enzyme (Fig. 3).

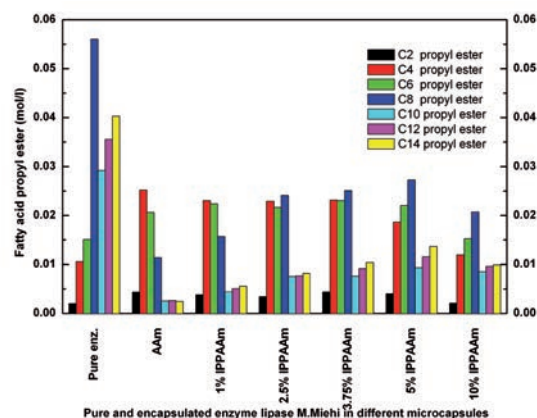


Figure 3: Reaction activity of free enzyme and encapsulated enzyme in different microcapsules.

The preceding results indicated that not only size exclusion but also hydrophobic-hydrophilic properties can be exploited using the permselective pAAm-Alg microcapsule membrane.

Publications:  
P.Pachariyanon, E.Barth,D.Agar, Enzyme immobilization in permselective microcapsule, Journal of microencapsulation, 28(5),370-383, August 2011

Contact:  
Pachariyanon.Pavadee@bci.tu-dortmund.de  
agar@bci.tu-dortmund.de

## Slug flow of ionic liquids in capillary microcontactors

*Internal circulation and mass transfer in a novel liquid-liquid extraction approach on small scale*

Frederik Scheiff, Alexander Holbach, David W. Agar

Slug flow in capillary micro reactors is an attractive option for implementing continuous liquid-liquid extraction with tailored ionic liquid solvents. However, efficient mass transfer relies on the internal circulation vortices within the liquid slugs. In which regime slug flow of ionic liquids can be established and how internal circulation and mass transfer are affected by the highly viscous ionic liquid has been investigated experimentally. Measures intended to enhance the limited circulation observed have been verified successfully.

Slug flow in microcapillaries is recognized as efficient technique for mass-transfer-limited operations like liquid-liquid extractions, because of interfacial diffusion collaborating with convective transport in Taylor vortices. Another facet of the process intensification philosophy in microreaction technology are ionic liquids. Due to their tunable solvent properties, ionic liquids have acquired an appreciable significance for industrial extraction processes.

In a first step, the operating window of organic-ionic liquid slug flow is established for 1-Ethyl-3-methylimidazolium alkylsulfates in a 1.0 mm ID plastic capillary.

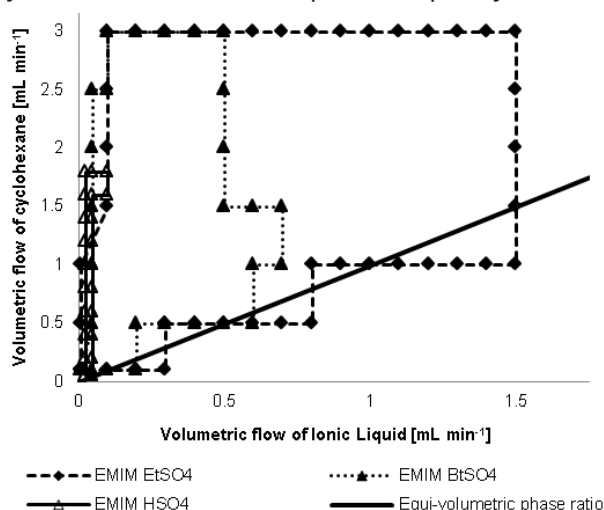


**Figure 1:** Operating windows of the slug flow micro capillary contactor as a function of flow rates for various liquids.

Two experimental key results can be deduced: the operating window narrows or even vanishes with increasing viscosity and an excess of the encapsulating organic medium is required.

The stability of slug flow is necessary, but not sufficient for the effectiveness of extraction in slug flow contactors. Compared to aqueous-organic systems, the convective

transport is damped by a factor of two to ten due to viscous effects in ionic liquids. But as proven by fluiddynamic investigations in EMIM ethylsulfate – n-heptane, these deficiencies can be compensated by increasing velocity, reducing viscosity by elevating the temperature and the choice of a wall material.

Eventually, the fluiddynamic contribution to mass transfer has been verified, as the extraction of acetic acid n-heptane with EMIM ethylsulfate, either by sole diffusion or by convective-diffusive transport in slug flow, is compared. The extraction is exhaustive owing to the solvent properties of ionic liquids in both cases. But slug flow allows for characteristic extraction times shorter by a factor of 170. As the specific surface area  $a$  is larger only by a factor of 28, evidence is provided that merely the distinct flow pattern in slug flow is sufficient to establish high mass transfer coefficients  $k_{l,a}$ .

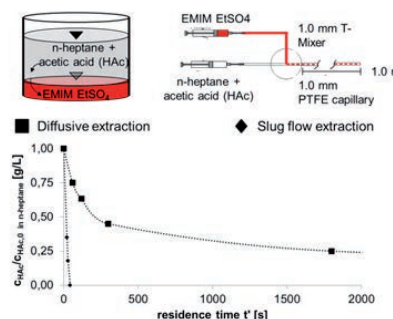


**Figure 2:** Extraction of acetic acid from n-heptane (raffinate) with EMIM EtSO<sub>4</sub> by a) pure diffusion, b) diffusion & superimposed convection in slug flow.

Hence, these results demonstrate the fluiddynamic feasibility of extraction in microcapillary slug flow with ionic liquids and may therefore provide an alternative for conventional and small scale extraction techniques

**Contact:**  
 frederik.scheiff@bci.tu-dortmund.de  
 alexander.holbach@bci.tu-dortmund.de  
 agar@bci.tu-dortmund.de

**Publications:**  
 F. Scheiff, V. Reimer, A. Holbach, D. W. Agar, Slug flow of ionic liquids in capillary microcontactors – internal circulation and mass transfer, IMRET 12 conference, Lyon, France (2012)



## Thermodynamics (TH)

## Solubility of Pharmaceuticals

### Novel approach for modeling pH-dependent solubility and salt formation

Jan Caßens, Anke Prudic, Feely Rüter, Gabriele Sadowski

Bioavailability of pharmaceuticals is very important for their therapeutic effect in the human body. It can be remarkably increased by salt formation, which can be achieved by adding an acid or a base and therewith also changing the pH. We measured the pH-dependent solubility of several pharmaceutical bases and observed that it strongly depends on the pH-changing substances. Applying a new modeling approach based on the ePC-SAFT equation of state the pH-dependent solubility as well as the salt formation could be described and even predicted.

The solubility of ionizable pharmaceuticals in aqueous solution strongly depends on the pH of the solution. As shown in Figure 1, the solubility of a pharmaceutical base, which is sparingly soluble at high pH, can be increased significantly by adding an acid to the solution, which lowers the pH.

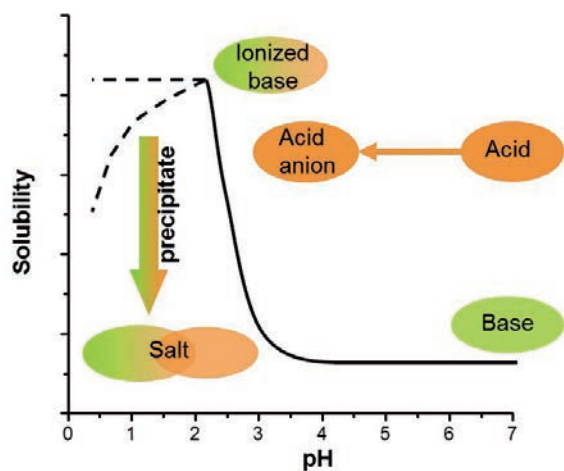


**Figure 1:** Schematic drawing of pH-dependent solubility for a pharmaceutical base.

The increase in solubility is caused by ionization of the pharmaceutical base leading to stronger interactions with the water molecules. Ionized cations of the pharmaceutical base and the acid anions form salts which are on their part limited in solubility and precipitate at a certain pH. Further decrease of pH thus may lead again to a decrease in solubility. The maximum in solubility and the trend of the solubility curve when salt precipitates (dashed lines in Figure 1) strongly depend on the type of acid used for pH modification as well as the salt precipitating.

Figure 2 shows the pH-dependent solubility profile for

lidocaine and thiabendazole. The measurements were performed at 298.15 K in a stirred reactor. The pH was shifted by adding hydrochloric acid or phosphoric acid, respectively.

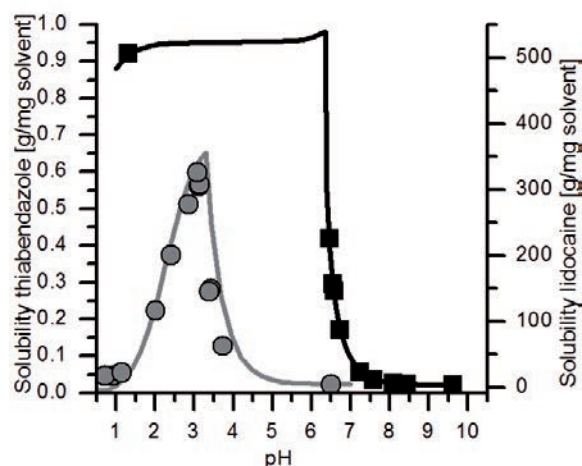


**Figure 2:** pH-dependent solubility of thiabendazole (gray) and lidocaine (black) at 298.15 K. Comparison between experimental data (symbols) and model results (lines). Hydrochloric acid (circles) and phosphoric acid (squares) were used for pH modification.

Applying a new modeling approach based on the ePC SAFT equation of state we were able to describe the pH-dependent solubility profile. The calculations were done only based on the knowledge of the dissociation constants, the solubility product of the salts and the binary interaction parameters which were fitted once to experimental solubility data at high pH. As shown in Figure 2 the modeling is in almost quantitative agreement with the experimental data. It demonstrates that the increasing solubility due to ion formation as well as the decreasing solubility at low pH is correct and even quantitatively captured by the model.

Publications:  
Caßens, J., Prudic, A., Rüter, F., Sadowski, G., Solubility of Pharmaceuticals and Their Salts as Function of pH, submitted to Journal of Pharmaceutical Science.

## Thermodynamic Characterization of Membrane Materials

### New Characterization Methodology to Predict Membrane Separation Efficiencies

Lisa Hesse, Gabriele Sadowski

Organic Solvent Nanofiltration (OSN) shows an enormous potential for the enrichment of high-value products, like pharmaceuticals, from an organic solvent stream at mild process conditions and low energy consumption. To predict the separation efficiency of OSN membranes, the materials were characterized thermodynamically by measuring the solubility and diffusion of organic solvents. Based on the subsequent modeling of these properties, fluxes through the OSN membrane could be predicted by means of a new flux model without further parameter fitting.

In order to obtain solubility and diffusion data, gravimetric sorption experiments were carried out. Two glassy polyimides, P84 and Matrimid (see Fig. 1), which are commonly used as OSN membrane materials, were investigated. As organic solvents four VOCs (volatile organic compounds) ethyl acetate, 2-propanol, ethanol, and toluene were chosen.

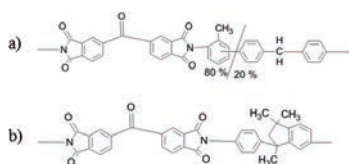


Figure 1: Monomer of a) P84 and b) Matrimid.

The solubility was modeled by the PC SAFT equation of state, which allows the estimation of all mixture properties, like the chemical potentials, needed for further flux modeling. The diffusion was modeled by an optimized Maxwell-Stefan diffusion model (see Fig. 2) by fitting diffusion coefficients to the measured sorption curves. For the consideration of the mechanical properties of the glassy polymers a viscoelastic model was used.

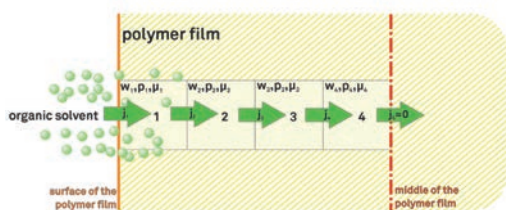


Figure 2: Schematic presentation of the model to calculate the organic solvent diffusion in a polymer film.

The obtained diffusion coefficients and the solubilities of all binary Matrimid/VOC systems are shown in Fig. 3. Due

to the different order of both values it can be stated that it is not possible to deduce one property from the other.

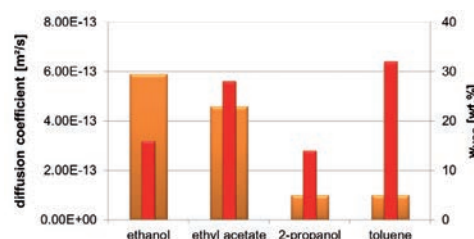


Figure 3: Diffusion coefficients (orange bars) and solubilities (red bars) of different VOCs in Matrimid.

Based on these data, a thermodynamically-based flux model was developed which allows the calculation of VOC fluxes through dense polymeric OSN-membranes based on the earlier-determined diffusion coefficients and chemical potentials without any time-consuming flow measurements. Figure 4 shows the good agreement of predicted and measured (Laboratory of Fluid Separations, J. Mićović and P. Schmidt) partial fluxes of the VOCs through an OSN Matrimid membrane.

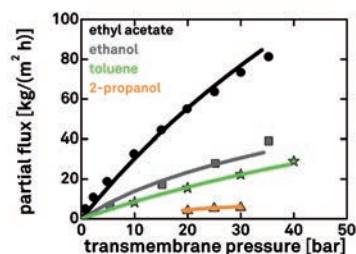


Figure 4: Measured (symbols) and modeled (lines) VOC fluxes through an OSN membrane made of Matrimid.

The prediction of the separation efficiency of OSN membranes makes this energy-efficient, product-friendly purification step accessible as an alternative way to traditional energy-intensive processes and will even allow the design of tailor-made membranes.

#### Publications:

Hesse L., Sadowski G., Modeling Liquid-Liquid Equilibria of Polyimide Solutions, Industrial & Engineering Chemistry Research, 51 (2012) 539 – 546

Hesse L., Naeem S., Sadowski G., VOC Sorption in Glassy Polyimides – Measurements and Modeling, Journal of Membrane Science, submitted

Hesse L., Mićović J., Schmidt P., Gorák A., Sadowski G., Modeling of VOC-Fluxes through a Polyimide Membrane, Journal of Membrane Science, submitted

#### Contact:

[lisa.hesse@tu-dortmund.de](mailto:lisa.hesse@tu-dortmund.de)

[g.sadowski@bci.tu-dortmund.de](mailto:g.sadowski@bci.tu-dortmund.de)



EUROPÄISCHE UNION  
Investition in unsere Zukunft  
Europäischer Fonds  
für regionale Entwicklung

Ziel2.NRW  
CheK.NRW

## Modeling Weak-Electrolyte Solutions

Thomas Reschke, Shahbaz Naeem, Gabriele Sadowski

The experimental determination and modeling of thermodynamic properties in weak-electrolyte solutions requires the knowledge of the dissociation equilibrium. In contrast to strong electrolytes, weak electrolytes exhibit a concentration dependence of the dissolved ionic species distribution. For the first time this effect is considered on both, experimental estimation and modeling of thermodynamic properties.

The dissociation equilibrium of acids and bases is a well examined phenomenon in chemistry and physics (Fig. 1). Applications of dissociation equilibria can, for example, be found in buffer solutions which combine an acid and its corresponding base.

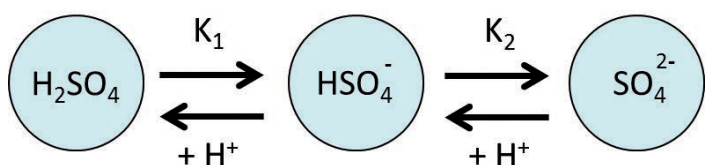


**Figure 1:** Dissociation equilibrium of sulfate species. The amount of dissolved ionic species is given by the dissociation constants  $K_{1/2}$ .

However, the consideration of the dissociation/association equilibrium in thermodynamic modeling is surprisingly quite uncommon. Weak electrolytes are often simply treated like strong ones neglecting the concentration-dependent species distribution.

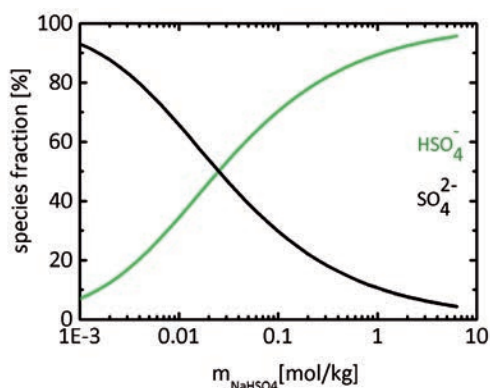


**Figure 2:** Species distribution of dissolved sulfate species as function of the initial salt ( $\text{NaHSO}_4$ ) concentration.

By examining the equilibrium concentrations of all dissolved species for  $\text{NaHSO}_4$  (Fig. 2) it could be shown, that this approach is insufficient, as the dissolved species

distribution is clearly changing with the concentration. This speciation has a strong effect on thermodynamic solution properties like the water activity coefficient  $\gamma_{\text{Water}}$ , which can be experimentally determined from vapor-pressure measurements. Applying the newly determined species distribution allows for calculating the true water activity coefficient. As Figure 3 shows, the newly calculated  $\gamma_{\text{speciation}}$  significantly differs from the erroneously determined  $\gamma_{\text{no speciation}}$ .

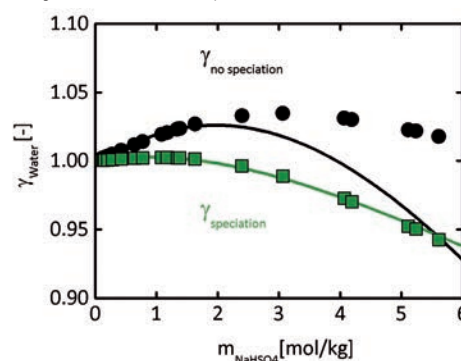


**Figure 3:** Water activity coefficient in an aqueous  $\text{NaHSO}_4$  solution. The symbols represent the experimentally determined activity coefficients, accounting for speciation and not accounting for speciation, respectively. The lines represent the respective ePC SAFT calculations.

Besides the improvement of experimental- data estimation we could show that the consideration of the species distribution in the modeling significantly improves the description of the (true) experimental data (Fig. 3). Applying this approach, the thermodynamic model ePC-SAFT allows for an almost quantitative modeling of phase equilibria (vapor-liquid or liquid-liquid) containing weak electrolytes.

Publications:  
Reschke T., Naeem S., Sadowski G., Osmotic Coefficients of Aqueous Weak Electrolyte Solutions: Influence of Dissociation on Data Reduction and Modeling, *Journal of Physical Chemistry B*, 2012, 116 (25), pp 7479–7491

## Decentralized Energy Supply for Domestic Applications

### Novel convertible Stirling – Vuilleumier hybrid system

Ingo Geue, Jens Pfeiffer, Hans-Detlev Kühl

As residential heating and warm water supply spans more than 40% of most industrialized countries end energy consumption (mainly fossil fuels), considerable savings can be achieved by decentralized combined heat and power production (CHP) and by heat pumps, preferably thermally driven ones. However, the fixed heat-to-power ratio presently impedes an ample dissemination of decentralized CHP, whereas heat pumps have to compete with conventional, low-cost heating systems. Regenerative cycles offer the unique opportunity of combining both a CHP system (Stirling engine) and a thermally driven Vuilleumier heat pump in just one convertible machine. Furthermore, a hybrid cycle with an intermediate power to heat ratio can be realized. So, this ratio can be adjusted to varying demand situations.

Figure 1 illustrates the three operation modes which can be realized in the convertible machine. The red color indicates a heat input at the hot temperature level (e.g. via fossil fuel), and the blue color a heat input at a low, typically ambient temperature level. These are converted into a heat rejection at the warm temperature level (green) which is considered to be useful heat (e.g. for space heating or warm water supply). Additionally, mechanical power (black) is produced in Stirling and hybrid operation.

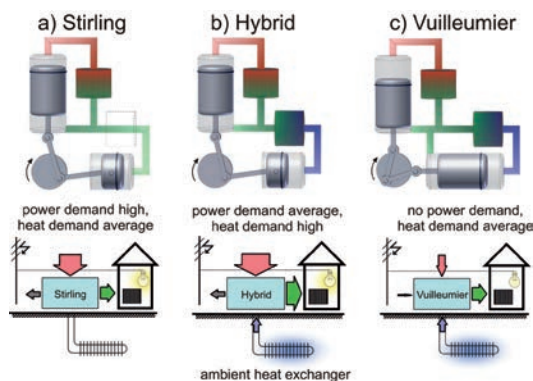


Figure 1: Operation modes of the convertible machine.

In a research project funded by the German Research Foundation (DFG), an application-oriented design of such a machine has been developed and optimized thermodynamically and economically. Subsequently, a laboratory-scale machine was derived from this design by similarity-based scaling (Figure 2).

This procedure yields a machine which can be realized and operated experimentally at a fraction of the effort required for the original design. Nevertheless, any relevant dimensionless numbers describing the gas cycle are preserved, including efficiencies and heat ratios in particular.



Figure 2: Photograph of the laboratory scale machine.

The experimental performance data can be reproduced satisfactorily by an existing simulation program developed at the Laboratory of Thermodynamics, when the losses caused by the experimental setup and the limitations of the scaling procedure are accounted for. As an example, Figure 3 illustrates this for three operating conditions in hybrid mode. So, it has been proven that the scale-down procedure is a valid means to reduce experimental efforts and that this convertible machine can be practically realized and therefore represents a promising concept as a future domestic energy supply system.

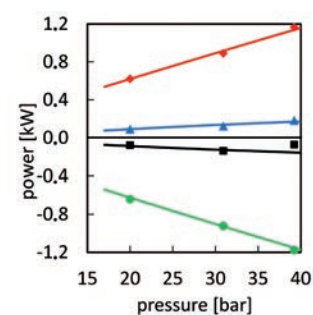


Figure 3: Thermal and mechanical power vs. mean operating pressure as measured (symbols) and simulated (lines) for hybrid operation at 300°C hot, 30°C warm and 5°C cold temperature level and 383 rpm speed

#### Contact:

ingo.geue@tu-dortmund.de

jens.pfeiffer@bci.tu-dortmund.de

hdk@bci.tu-dortmund.de

#### Publications:

Kühl, H.-D.; Geue, I.: Application of Similarity-Based Scaling to the Design of an Experimental, Laboratory-Scale Convertible Stirling-Vuilleumier Hybrid Engine, Proc. 7th IECEC, Denver, 2009  
Geue, I.; Pfeiffer, J.; Kühl, H.-D.: Experimental Results of a Novel Laboratory-Scale Stirling-Vuilleumier Hybrid System, Proc. 9th IECEC, San Diego, 2011

### **Impressum**

Fakultät Bio- und Chemieingenieurwesen  
der Technischen Universität Dortmund

Prof. Jörg C. Tiller

Emil-Figge-Str. 70

44227 Dortmund

[www.bci.tu-dortmund.de](http://www.bci.tu-dortmund.de)

**SCIENTIFIC**

**HIGHLIGHTS**